Quantum Sensors

G J Milburn.
University of Susssex

January 9, 2025

1. Clocks

2. Quantum parameter estimation.

3. Atom Sensors

What is a clock?

Thermodynamics of clocks.

All clocks, classical and quantum, are irreversible systems pushed away from equilibrium.

Thermodynamics of clocks.

All clocks, classical and quantum, are irreversible systems pushed away from equilibrium.

Free energy:

$$\Delta F = \Delta E - T\Delta S$$

Thermodynamics of clocks.

All clocks, classical and quantum, are irreversible systems pushed away from equilibrium.

Free energy:

$$\Delta F = \Delta E - T\Delta S$$

$\Delta F > 0$, do work to increase E

Make measurements to decrease S

Thermodynamics of clocks.

All clocks, classical and quantum, are irreversible systems pushed away from equilibrium.

Free energy:

$$\Delta F = \Delta E - T\Delta S$$

$\Delta F > 0$, do work to increase E
Make measurements to decrease S

See GJM The thermodynamics of clocks, Contemporary Physics, 2020.

Work driven clocks and limit cycles .

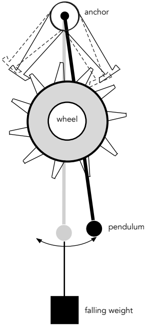

Pendulum clock: a driven non linear oscillator in a non equilibrium steady state.

Work driven clocks and limit cycles .

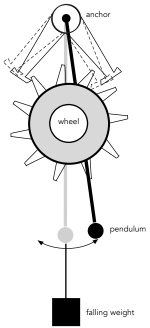

Pendulum clock: a driven non linear oscillator in a non equilibrium steady state.

The steady state is a limit cycle, a one dimensional attractor.

Work driven clocks and limit cycles .

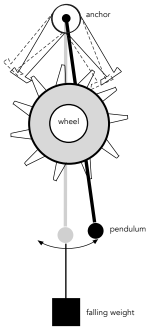

Pendulum clock: a driven non linear oscillator in a non equilibrium steady state.

The steady state is a limit cycle, a one dimensional attractor.

See GJM The thermodynamics of clocks, Contemporary Physics 2020.

Work driven clocks and limit cycles .

Equations of motion:

$$\begin{aligned}\dot{x} &= y \\ \dot{y} &= -x - \Gamma y + K(x,y) + \eta(t)\end{aligned}$$

Γ damping, $\eta(t)$ a delta correlated Langevin noise force.

Work driven clocks and limit cycles .

Equations of motion:

$$\begin{aligned} \dot{x} &= y \\ \dot{y} &= -x - \Gamma y + K(x,y) + \eta(t) \end{aligned}$$

Γ damping, $\eta(t)$ a delta correlated Langevin noise force.

Adiabatic elimination of the ratchet dynamics to define the 'kick function'

$$K(x,y) = -\mu \, \mathrm{sign}(\sin\psi_0 \, x - \cos\psi_0 \, y)$$

ψ_0 is fixed by the design of the escapement and μ has units of frequency.

Work driven clocks and limit cycles .

On the limit cycle (with no noise):

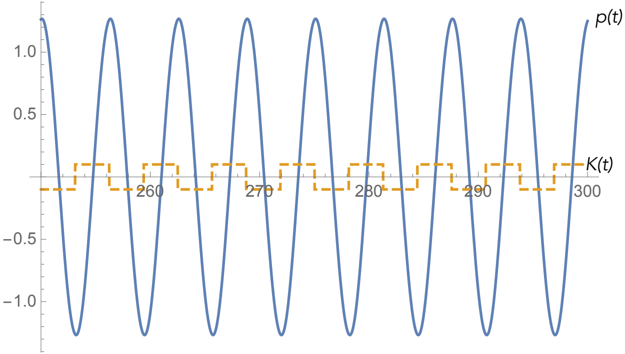

Angular momentum (solid) and the impulse function (dashed) versus time for the kicked pendulum with $\sin\psi_0 = 0.1$ $\Gamma = 0.1$ $\mu = 0.1$.

Limit cycles .

On each cycle, work done by drive equals energy dissipated.

Limit cycles .

On each cycle, work done by drive equals energy dissipated.

The larger the limit cycle, the greater the power dissipated.

Limit cycles .

Polar coordinates $x = r\cos\theta, y = r\sin\theta$.

Limit cycles .

Polar coordinates $x = r\cos\theta, y = r\sin\theta$.

$$
\begin{aligned}
\frac{dr}{dt} &= -\frac{\Gamma r}{2} + \frac{2\mu}{\pi}\cos\psi_0 \\
\frac{d\theta}{dt} &= -1 + \frac{2\mu}{r\pi}\sin\psi_0
\end{aligned}
$$

Limit cycles .

Polar coordinates $x = r\cos\theta, y = r\sin\theta$.

$$\begin{aligned} \frac{dr}{dt} &= -\frac{\Gamma r}{2} + \frac{2\mu}{\pi}\cos\psi_0 \\ \frac{d\theta}{dt} &= -1 + \frac{2\mu}{r\pi}\sin\psi_0 \end{aligned}$$

fixed point

$$r_* = \frac{4\mu}{\Gamma\pi}\cos\psi_0$$

recall μ is the driving strength.

Limit cycles with thermal noise.

Ito stochastic diferential equations

$$
\begin{aligned}
dr &= [-\frac{\Gamma r}{2} + \frac{2\mu}{\pi}\cos\psi_0 + \frac{D}{4r}]dt + \sqrt{D/2}\, dW_1(t) \\
d\theta &= [-1 + \frac{2\mu}{r\pi}\sin\psi_0]dt + \frac{\sqrt{D/2}}{r}\, dW_2(t)
\end{aligned}
$$

$dW_1(t), dW_2(t)$, independent Wiener increments
diffusion constant $D = \frac{2\omega\gamma k_B T}{mg^2}$

Limit cycles with thermal noise.

Ito stochastic diferential equations

$$
\begin{aligned}
dr &= [-\frac{\Gamma r}{2} + \frac{2\mu}{\pi}\cos\psi_0 + \frac{D}{4r}]dt + \sqrt{D/2}\, dW_1(t) \\
d\theta &= [-1 + \frac{2\mu}{r\pi}\sin\psi_0]dt + \frac{\sqrt{D/2}}{r}\, dW_2(t)
\end{aligned}
$$

$dW_1(t), dW_2(t)$, independent Wiener increments
diffusion constant $D = \frac{2\omega\gamma k_B T}{mg^2}$

Linearise phase noise on limit cycle $r = r_*$

$$
d\theta = [-1 + \frac{2\mu}{r_*\pi}\sin\psi_0]dt + \frac{\sqrt{D'/2}}{r_*}\, dW_2(t)
$$

Limit cycles with thermal noise.

Ito stochastic diferential equations

$$
\begin{aligned}
dr &= [-\frac{\Gamma r}{2} + \frac{2\mu}{\pi}\cos\psi_0 + \frac{D}{4r}]dt + \sqrt{D/2}\, dW_1(t) \\
d\theta &= [-1 + \frac{2\mu}{r\pi}\sin\psi_0]dt + \frac{\sqrt{D/2}}{r}\, dW_2(t)
\end{aligned}
$$

$dW_1(t), dW_2(t)$, independent Wiener increments
diffusion constant $D = \frac{2\omega\gamma k_B T}{mg^2}$

Linearise phase noise on limit cycle $r = r_*$

$$
d\theta = [-1 + \frac{2\mu}{r_*\pi}\sin\psi_0]dt + \frac{\sqrt{D'/2}}{r_*}\, dW_2(t)
$$

Phase noise gets smaller the larger the limit cycle.

Noise and fluctuations in period.

On the limit cycle

$$K(t) = -\mu r_* \,\mathrm{sign}[\cos(\theta(t) + \psi_0)]$$

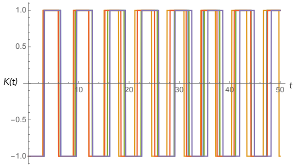

Noise and fluctuations in period.

On the limit cycle

$$K(t) = -\mu r_* \,\mathrm{sign}[\cos(\theta(t) + \psi_0)]$$

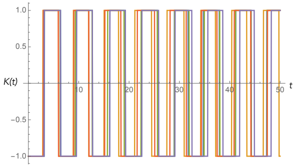

Time take for $\theta(t) + \psi_0 = 2\pi$ is a random variable. The period fluctuates from cycle to cycle.

Noise and fluctuations in period.

On the limit cycle

$$K(t) = -\mu r_* \operatorname{sign}[\cos(\theta(t) + \psi_0)]$$

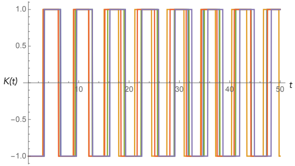

Time take for $\theta(t) + \psi_0 = 2\pi$ is a random variable. The period fluctuates from cycle to cycle.

A 'first passage time' problem

Noise and fluctuations in period.

The distribution of periods follows an inverse Gaussian distribution

$$p(T) = \sqrt{\frac{2\pi r_*}{\sigma T^3}} \exp\left(-\frac{r_*(2\pi - \omega T)^2}{2\sigma T}\right)$$

Noise and fluctuations in period.

The distribution of periods follows an inverse Gaussian distribution

$$p(T) = \sqrt{\frac{2\pi r_*}{\sigma T^3}} \exp\left(-\frac{r_*(2\pi - \omega T)^2}{2\sigma T}\right)$$

The mean and variance

$$\begin{aligned} E[T] &= \frac{2\pi}{\omega} \\ Var[T] &= \frac{2\pi\sigma}{\omega^3 r_*} \end{aligned}$$

where $\sigma = D/2 \propto$ temperature.

The larger the limit cycle, the more regular the clock signal.

Noise and fluctuations in period.

The distribution of periods follows an inverse Gaussian distribution

$$p(T) = \sqrt{\frac{2\pi r_*}{\sigma T^3}} \exp\left(-\frac{r_*(2\pi - \omega T)^2}{2\sigma T}\right)$$

The mean and variance

$$\begin{aligned} E[T] &= \frac{2\pi}{\omega} \\ Var[T] &= \frac{2\pi\sigma}{\omega^3 r_*} \end{aligned}$$

where $\sigma = D/2 \propto$ temperature.

The larger the limit cycle, the more regular the clock signal.

Good clocks are necessarily dissipative.

Electronic clocks.

Quartz piezo-electric crystal in a feedback circuit to: Schmidtt trigger.

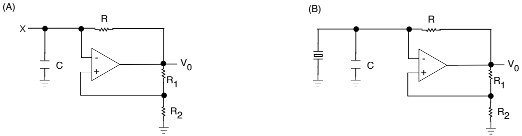

Figure: (A). A Schmidtt trigger Op Amp. with feedback configured as an astable oscillator (B) A quartz piezo electric oscillator coupled to an astable oscillator

Electronic clocks.

Quartz piezo-electric crystal in a feedback circuit to: Schmidtt trigger.

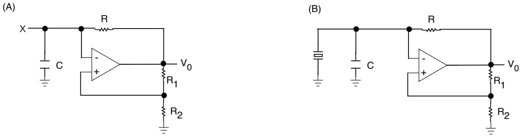

Figure: (A). A Schmidtt trigger Op Amp. with feedback configured as an astable oscillator (B) A quartz piezo electric oscillator coupled to an astable oscillator

The Op Amp is configured as a comparator.

Electronic clocks.

A phenomenological model:

$$\begin{aligned}\dot{V} &= \gamma(1-g(V))e^{-\eta X} - \gamma(1+g(V))e^{\eta X} \\ \dot{X} &= \omega Y \\ \dot{Y} &= -\omega X - \kappa Y + \chi V\end{aligned}$$

where V, output voltage of the Schmidtt trigger, X voltage on capacitor and Y is the flux in inductor, ω is the natural frequency of the equivalent LC circuit.

Gain function:

$$g(V) = \frac{V + \tanh \beta V}{1 + V \tanh \beta V}$$

feedback ratio: $\beta = R_1/(R_1 + R_2)$.

Electronic clocks.

The limit cycle occurs via a Hopf bifurcation for values of χ above a critical value where the fixed point at the origin becomes unstable.

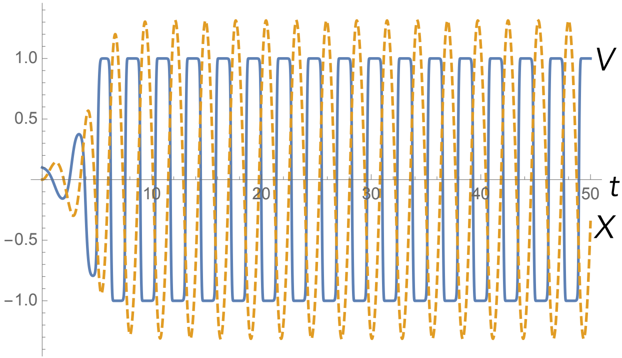

$\omega = 1, \gamma = 0.1$, $\eta = 8.0$, $\kappa = 1.0$, $\beta = 1.0$ and $\chi = 5.0$.

Electronic clocks at microwave frequencies.

A Gunn diode: controllable negative resistance (amplification) above a threshold voltage applied DC voltage. Produces electronic oscillations on a limit cycle at microwave frequencies.

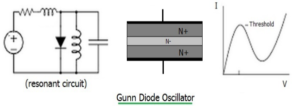

https://www.rfwireless-world.com/

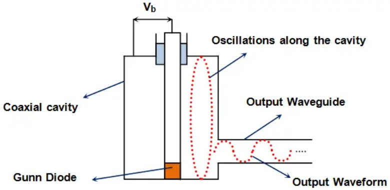

https://www.electrical4u.com/

Electronic clocks at microwave frequencies.

Counter circuit.

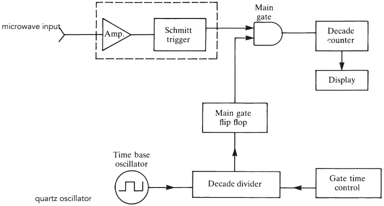

Fig. 10.1 Basic frequency counter.

https://link.springer.com/chapter/10.1007/978-94-011-6950-9_10

Schmitt trigger converts the input signal into rectangular pulses of the same repetition frequency. The pulses are then counted by a decade counting assembly and displayed. The number of pulses allowed to be counted depends on the time for which the main gate is opened by the time-base circuitry. The ratio of the number of pulses counted to the known maingate- ON time is the frequency of the input signal.

Clock design.

1. a component that will produce a "periodic phenomenon." We shall call this device a **resonator**.
2. We must sustain the periodic motion by feeding energy to the resonator. We shall call the resonator and the energy source, taken together, an **oscillator**.
3. Means for counting the periods.

see: *From sundials to atomic clocks* James Jespersen and Jane Fitz-Randolph
`https://www.govinfo.gov/content/pkg/GOVPUB-C13-755d634ef7c0cb8066a95740208a72f3/pdf/GOVPUB-C13-755d634ef7c0cb8066a95740208a72f3.pdf`

Physical time is relational.

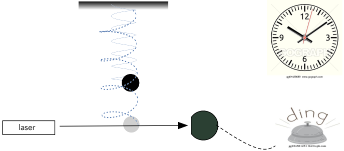

v	n
0	1
0	2
0	3
1	4
0	5
0	6
0	7
0	8
1	9
0	10
0	11
0	12
0	1
1	2
0	3
0	4
0	5
0	6
1	7
0	8
0	9

Clocks measure coincidences between local events, **here and now**.

Physical time is relational.

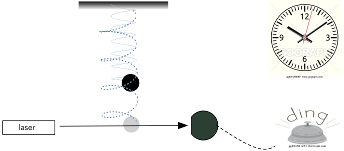

v	n
0	1
0	2
0	3
1	4
0	5
0	6
0	7
0	8
1	9
0	10
0	11
0	12
0	1
1	2
0	3
0	4
0	5
0	6
1	7
0	8
0	9

Clocks measure coincidences between local events, **here and now**.

Must specify the temperature of the local environment to define the clock. (Tolman relations in GR)

Physical time is relational.

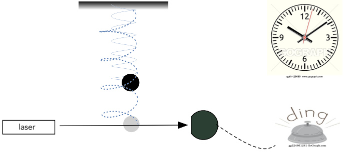

v	n
0	1
0	2
0	3
1	4
0	5
0	6
0	7
0	8
1	9
0	10
0	11
0	12
0	1
1	2
0	3
0	4
0	5
0	6
1	7
0	8
0	9

Clocks measure coincidences between local events, **here and now**.

Must specify the temperature of the local environment to define the clock. (Tolman relations in GR)

A clock record is a count $n \in \mathbb{N}$.

Physical time is relational.

https://www.dropbox.com/s/3wpj9pa0s038u8d/sound-clock.m4v?dl=0

Physical time is relational.

Event-count coincidences.

n	ν
1	1
2	0
3	1
4	0
5	0
6	0
7	1
8	0
9	1

$\nu(n)$

Physical time is relational.

Units?

Physical time is relational.

Units?

Give a particular clock, you can define "one unit " of time as a total count of M.

Physical time is relational.

Units?

Give a particular clock, you can define "one unit " of time as a total count of M.

Example:

$$N = 9,192,631,770$$

ticks of the atomic Cs clock is called ‘one second’.

Physical time is relational.

Example: deterministic recurring event that either occurs or does not occur at some clock count,

$$\nu : \mathbb{N} \to \{0, 1\}$$

Physical time is relational.

Example: deterministic recurring event that either occurs or does not occur at some clock count,

$$\nu : \mathbb{N} \rightarrow \{0, 1\}$$

If the clock is perfect, $\exists a \in \mathbb{N}$ such that $\nu(n + a) = \nu(n)$.

Physical time is relational.

Example: deterministic recurring event that either occurs or does not occur at some clock count,

$$\nu : \mathbb{N} \to \{0, 1\}$$

If the clock is perfect, $\exists a \in \mathbb{N}$ such that $\nu(n + a) = \nu(n)$.

There are no perfect clocks,

$$\nu(n|\sigma) = \begin{cases} 1 & n \bmod N = 0 \\ 0 & n \bmod N = 1 \end{cases}$$

with N a random integer with mean a and variance σ.

Physical time is relational.

Example: deterministic recurring event that either occurs or does not occur at some clock count,

$$\nu : \mathbb{N} \to \{0, 1\}$$

If the clock is perfect, $\exists a \in \mathbb{N}$ such that $\nu(n + a) = \nu(n)$.

There are no perfect clocks,

$$\nu(n|\sigma) = \begin{cases} 1 & n \bmod N = 0 \\ 0 & n \bmod N = 1 \end{cases}$$

with N a random integer with mean a and variance σ.

Define a count function.

$$C(n) = \sum_{k=1}^{n} \nu(k)$$

Physical time is relational.

Parametric representation;

$$\{\nu(t), n(t)\}$$

where $t \in \mathbb{R}$.

Physical time is relational.

Parametric representation;

$$\{\nu(t), n(t)\}$$

where $t \in \mathbb{R}$.

The parameter t has no physical significance. Only the relation of coincidences between physical events, $\nu(n)$, has physical significance.

Physical time is relational.

Real parameterisation $t \in \mathbb{R}$ then $\nu(n) \rightarrow (\nu(t), n(t))$

Physical time is relational.

Real parameterisation $t \in \mathbb{R}$ then $\nu(n) \to (\nu(t), n(t))$

Example: define a count function $C : \mathbb{R} \to \mathbb{N}$

$$
\begin{aligned}
n(t) &= [t] \\
C(t) &= \left[\frac{t}{a}\right]
\end{aligned}
$$

where $[t]$ is integer part.

Physical time is relational.

Real parameterisation $t \in \mathbb{R}$ then $\nu(n) \to (\nu(t), n(t))$

Example: define a count function $C : \mathbb{R} \to \mathbb{N}$

$$\begin{aligned} n(t) &= [t] \\ C(t) &= \left[\frac{t}{a}\right] \end{aligned}$$

where $[t]$ is integer part.
Shift the origin $m = n - [a]$,

$$\nu(m) = \begin{cases} 1 & m \bmod [a] = 0 \\ 0 & m \bmod [a] = 1 \end{cases}$$

Physical time is relational.

The relation $\nu(n)$ refers to space-time events independent of reference frames. It is coordinate free.

Physical time is relational.

The relation $\nu(n)$ refers to space-time events independent of reference frames. It is coordinate free.

All spacetime events are the results of physical measurements.

Physical time is relational.

The relation $\nu(n)$ refers to space-time events independent of reference frames. It is coordinate free.

All spacetime events are the results of physical measurements.

The real parameterisation of local correlations, $(\nu(t), n(t))$, depends on the gravitational field.

What we measure when we ‘measure’ time.

Mach,1911:

> *We can eliminate time from every law of nature by putting in its place a phenomenon dependent on the earth’s angle of rotation .... Physically, then, time is the representability of any phenomenon as a function of any other one.*

What we measure when we ‘measure’ time.

Rovelli, 2004:

> *The fundamental equations do not include a time variable, but they do include variables that change in relation to each other. Time, as Aristotle suggested, is the measure of* **change***: different variables can be chosen to measure that change, and none of these has ALL the characteristics of time as we perceive it. But this does not alter the fact that the world is a ceaseless process of change.*

Noise and fluctuations in period.

Generic form:

$$W(t,\alpha,\lambda) = \sqrt{\frac{\lambda}{2\pi}}\, t^{-3/2} \exp\left[-\frac{\lambda}{2\mu^2 t}(t-\alpha)^2\right] \qquad t \geq 0 \ ,$$

where α, λ are positive real parameters (λ is called the spread parameter).

Noise and fluctuations in period.

Generic form:

$$W(t,\alpha,\lambda)=\sqrt{\frac{\lambda}{2\pi}}t^{-3/2}\exp\left[-\frac{\lambda}{2\mu^2 t}(t-\alpha)^2\right] \qquad t\geq 0\ ,$$

where α, λ are positive real parameters (λ is called the spread parameter).

Determined by the mean and variance as

$$\begin{aligned}\overline{T} &= \alpha \\ \overline{\Delta T^2} &= \frac{\alpha^3}{\lambda}\ .\end{aligned}$$

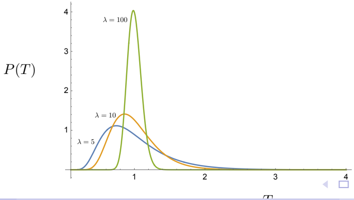

Noise and fluctuations in period.

Property of divisibility.

If T is a random variable with a Wald distribution with mean α and spread parameter λ then there exist n pieces of i.i.d. random variable $T_1, T_2, ..., T_n$ each from the Wald distribution with mean α/n and spread parameter λ/n such that $T \equiv T_1 + T_2 + ... + T_n$.

Noise and fluctuations in period.

Property of divisibility.

If T is a random variable with a Wald distribution with mean α and spread parameter λ then there exist n pieces of i.i.d. random variable $T_1, T_2, \ldots, T_n$ each from the Wald distribution with mean α/n and spread parameter λ/n such that $T \equiv T_1 + T_2 + \ldots + T_n$.

Each sample period T_k in a ticking clock is independent.

Noise and fluctuations in period.

Property of divisibility.

If T is a random variable with a Wald distribution with mean α and spread parameter λ then there exist n pieces of i.i.d. random variable $T_1, T_2, ..., T_n$ each from the Wald distribution with mean α/n and spread parameter λ/n such that $T \equiv T_1 + T_2 + ... + T_n$.

Each sample period T_k in a ticking clock is independent.

The stochastic history of a particular clock: total count, N, and the list of periods $T_1, T_2, \ldots T_N$.

T_N is Wald distributed, mean and spread $N\alpha, N\lambda$.

Noise and fluctuations in period.

The total elapsed parametric time is

$$t_N = \sum_{k=1}^{N} T_k$$

The mean of T_N is $N\alpha$ and the variance is

$$\Delta^2 \equiv \overline{\Delta T_N^2} = N^2 \frac{\alpha^3}{\lambda}$$

If we define the signal to noise ratio:

$$SNR = \frac{\bar{T}_N}{\Delta} = \sqrt{\frac{\lambda}{\alpha}}$$

independent of the total count, N.

Comparing clocks.

Two independent clocks, A and B, with the same values of α, λ.

Comparing clocks.

Two independent clocks, A and B, with the same values of α, λ.

We regard clock A as the relational clock for coordinating the tick events in clock B.

Comparing clocks.

Two independent clocks, A and B, with the same values of α, λ.

We regard clock A as the relational clock for coordinating the tick events in clock B.

when A records a count of N, the number of events, M, recorded in clock B is not necessarily the same.

Comparing clocks.

Two independent clocks, A and B, with the same values of α, λ.

We regard clock A as the relational clock for coordinating the tick events in clock B.

when A records a count of N, the number of events, M, recorded in clock B is not necessarily the same.

Error : $\epsilon(M) = (1 - M/N)^2$.

Comparing clocks.

Two independent clocks, A and B, with the same values of α, λ.

We regard clock A as the relational clock for coordinating the tick events in clock B.

when A records a count of N, the number of events, M, recorded in clock B is not necessarily the same.

Error : $\epsilon(M) = (1 - M/N)^2$. The average error for $\alpha = 1$

$$\bar{\epsilon} = \frac{1}{\lambda}$$

The average error decreases as thermal noise decreases.

Comparing clocks.

Define the integer valued function $N_A(t)$

$$N_A(t) = \left\lfloor \frac{t}{\alpha} \right\rfloor$$

Comparing clocks.

Define the integer valued function $N_A(t)$

$$N_A(t) = \left\lfloor \frac{t}{\alpha} \right\rfloor$$

If $N_A(t_N) = N$, write $t_N = N\alpha$.

Comparing clocks.

Define the integer valued function $N_A(t)$

$$N_A(t) = \left\lfloor \frac{t}{\alpha} \right\rfloor$$

If $N_A(t_N) = N$, write $t_N = N\alpha$.

$$P(M = N) = \int_0^{(N+1)/\mu} dt\ W(t, M\alpha, M\lambda) - \int_0^{(N-1)/\mu} dt\ W(t, M\alpha, M\lambda)$$

Comparing clocks.

Define the integer valued function $N_A(t)$

$$N_A(t) = \left\lfloor \frac{t}{\alpha} \right\rfloor$$

If $N_A(t_N) = N$, write $t_N = N\alpha$.

$$P(M = N) = \int_0^{(N+1)/\mu} dt\ W(t, M\alpha, M\lambda) - \int_0^{(N-1)/\mu} dt\ W(t, M\alpha, M\lambda)$$

The average error for $\alpha = 1$

$$\bar{\epsilon} = \frac{1}{\lambda} \tag{1}$$

which decreases as the spread parameter increases. The average error decreases as thermal noise decreases.

Comparing clocks.

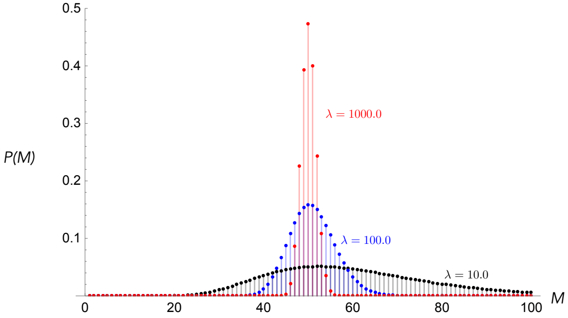

The probability that clock B counts M when clock A has a count of $N = 50$, and We set $\alpha = 1.0$.

Comparing clocks.

A clock is a counter, but can assign arbitrary units:

The second is currently defined as the time interval realized by counting $N = 9192631770$ *cycles of the frequency associated with the hyperfine transition in the ground state of an unperturbed cesium* 133 *atom.*

Quantum limit cycles.

At very low temperature, **dissipation** requires quantum noise to preserve unitarity.

Quantum limit cycles.

At very low temperature, **dissipation** requires quantum noise to preserve unitarity.

At very low temperature, **amplification** requires quantum noise to preserve unitarity.

Quantum clocks are irreversible and noisy due to quantum noise at very low temperature.

Quantum limit cycles.

At very low temperature, **dissipation** requires quantum noise to preserve unitarity.

At very low temperature, **amplification** requires quantum noise to preserve unitarity.

Quantum clocks are irreversible and noisy due to quantum noise at very low temperature.

Explicitly include continuous measurement.

Example: the laser.

A laser is a quantum clock, if you add a counter.

Example: the laser.

A laser is a quantum clock, if you add a counter.

Operates between a high temperature and a low temperature reservoir to maintain a population inversion.

Example: the laser.

A laser is a quantum clock, if you add a counter.

Operates between a high temperature and a low temperature reservoir to maintain a population inversion.

Simple dissipative nonlinear oscillator

$$\dot{\rho} = G n_s \mathcal{D}[a^\dagger] \left(\mathcal{A}[a^\dagger] + n_s\right)^{-1} \rho + \kappa \mathcal{D}[a]\rho$$

$$\begin{aligned} \mathcal{D}[B]\rho &= B\rho B^\dagger - \frac{1}{2}(A^\dagger A\rho + \rho A^\dagger A) \\ \mathcal{A}[B]\rho &= \frac{1}{2}(B^\dagger B\rho + \rho B^\dagger B) \end{aligned}$$

G is the small signal gain, n_s saturation photon number and κ is the cavity decay rate.

Equivalent classical model

Dynamics of the average field $\alpha(t) = \mathrm{tr}(a\rho(t))$

$$\dot{\alpha} = -\frac{\kappa\alpha}{2}\left(1 - \frac{Gn_s}{\kappa(|\alpha|^2 + n_s)}\right)$$

Well above threshold this is similar to the van der Pol oscillator in a rotating frame.

There are two fixed points $\alpha_0 = 0$ and $|\alpha_0|^2 = Gn_s/\kappa$ for $G >> \kappa$. The second solution is the above threshold limit-cycle solution.

Quantum model

Photon number distribution: $p_n(t) = \langle n|\rho(t)|n\rangle$.

$$\frac{dp_n(t)}{dt} = Gn_s\left[\frac{n}{n+n_s}p_{n-1} - \frac{n+1}{n+1+n_s}p_n\right] + \kappa(n+1)p_{n+1} - \kappa np_n$$

Quantum model

Photon number distribution: $p_n(t) = \langle n|\rho(t)|n\rangle$.

$$\frac{dp_n(t)}{dt} = Gn_s\left[\frac{n}{n+n_s}p_{n-1} - \frac{n+1}{n+1+n_s}p_n\right] + \kappa(n+1)p_{n+1} - \kappa n p_n$$

The steady state solution:

$$p_n^{ss} = \mathcal{N}\frac{(Gn_s/\kappa)^{n+n_s}}{(n+n_s)!}$$

Quantum model

Photon number distribution: $p_n(t) = \langle n|\rho(t)|n\rangle$.

$$\frac{dp_n(t)}{dt} = Gn_s\left[\frac{n}{n+n_s}p_{n-1} - \frac{n+1}{n+1+n_s}p_n\right] + \kappa(n+1)p_{n+1} - \kappa n p_n$$

The steady state solution:

$$p_n^{ss} = \mathcal{N}\frac{(Gn_s/\kappa)^{n+n_s}}{(n+n_s)!}$$

Below threshold $G < \kappa$,

$$p_n^{ss} \approx \frac{1}{1+\bar{n}}\left(\frac{\bar{n}}{\bar{n}+1}\right)^n \qquad G < \kappa$$

which is analogous to a thermal distribution with

$$\bar{n} = \frac{G}{\kappa - G}$$

Quantum model

Photon number distribution: $p_n(t) = \langle n|\rho(t)|n\rangle$.

$$\frac{dp_n(t)}{dt} = Gn_s\left[\frac{n}{n+n_s}p_{n-1} - \frac{n+1}{n+1+n_s}p_n\right] + \kappa(n+1)p_{n+1} - \kappa n p_n$$

The steady state solution:

$$p_n^{ss} = \mathcal{N}\frac{(Gn_s/\kappa)^{n+n_s}}{(n+n_s)!}$$

Below threshold $G < \kappa$,

$$p_n^{ss} \approx \frac{1}{1+\bar{n}}\left(\frac{\bar{n}}{\bar{n}+1}\right)^n \qquad G < \kappa$$

which is analogous to a thermal distribution with

$$\bar{n} = \frac{G}{\kappa - G}$$

Well above threshold $G >> \kappa$ the steady state distribution is Poisson with mean $\bar{n} = Gn_s/\kappa$

Quantum model

What to measure?

Quantum model

What to measure?

Photon counting ? .... a Poisson distribution of counts. No oscillatory clock signal.

Quantum model

What to measure?

Photon counting ? .... a Poisson distribution of counts. No oscillatory clock signal.

No point in measuring output intensity.

Quantum model

Howard Wiseman:

“Light amplification without stimulated emission: Beyond the standard quantum limit to the laser linewidth",Phys. Rev. A, 60, 4083

“Stochastic quantum dynamics of a continuously monitored laser", Phys. Rev. A, 47, 5180.

Quantum model: phase diffusion.

Quantum noise on the limit cycle:

$$\dot{\rho} = \Gamma\mathcal{D}[a^\dagger a]\rho$$

quantum phase diffusion at rate

$$\Gamma = \kappa/2\bar{n}$$

Quantum model: phase diffusion.

Quantum noise on the limit cycle:

$$\dot{\rho} = \Gamma\mathcal{D}[a^\dagger a]\rho$$

quantum phase diffusion at rate

$$\Gamma = \kappa/2\bar{n}$$

Phase diffusion rate decreases with the size of the limit cycle.

Quantum model: phase diffusion.

Quantum noise on the limit cycle:

$$\dot{\rho} = \Gamma \mathcal{D}[a^\dagger a]\rho$$

quantum phase diffusion at rate

$$\Gamma = \kappa/2\bar{n}$$

Phase diffusion rate decreases with the size of the limit cycle.

Energy dissipated by cavity loss is $\propto \kappa\bar{n}$.

Quantum model: phase diffusion.

Quantum noise on the limit cycle:

$$\dot{\rho} = \Gamma \mathcal{D}[a^\dagger a]\rho$$

quantum phase diffusion at rate

$$\Gamma = \kappa/2\bar{n}$$

Phase diffusion rate decreases with the size of the limit cycle.

Energy dissipated by cavity loss is $\propto \kappa\bar{n}$.

Good clock dissipates more power.

Quantum model: phase diffusion.

Additional notes on phase diffusion.

Quantum model: phase diffusion.

Additional notes on phase diffusion.

consider simple harmonic oscillator undergoing a time evolution for a random time T ... one period of a noisy clock

Quantum model: phase diffusion.

Additional notes on phase diffusion.

consider simple harmonic oscillator undergoing a time evolution for a random time T ... one period of a noisy clock

$$\rho(T) = e^{-i\omega T a^\dagger a}\rho(0)e^{i\omega T a^\dagger a}$$

Quantum model: phase diffusion.

Additional notes on phase diffusion.

consider simple harmonic oscillator undergoing a time evolution for a random time T ... one period of a noisy clock

$$\rho(T) = e^{-i\omega T a^\dagger a}\rho(0)e^{i\omega T a^\dagger a}$$

Average over times T

$$\mathcal{E}(\rho) = \int_0^\infty dT\ P(T)e^{-i\omega T a^\dagger a}\rho(0)e^{i\omega T a^\dagger a}$$

Quantum model: phase diffusion.

Additional notes on phase diffusion.

consider simple harmonic oscillator undergoing a time evolution for a random time T ... one period of a noisy clock

$$\rho(T) = e^{-i\omega T a^\dagger a}\rho(0)e^{i\omega T a^\dagger a}$$

Average over times T

$$\mathcal{E}(\rho) = \int_0^\infty dT\ P(T)e^{-i\omega T a^\dagger a}\rho(0)e^{i\omega T a^\dagger a}$$

$$\langle n|\mathcal{E}(\rho)|m\rangle = \int_0^\infty dT\ P(T)e^{-i\omega T(n-m)}\langle n|\rho(0)|m\rangle$$

Quantum model: phase diffusion.

Additional notes on phase diffusion.

Quantum model: phase diffusion.

Additional notes on phase diffusion.

Assume Wald distribution:

$$P(T) = \sqrt{\frac{\lambda}{2\pi T^3}} \exp\left[-\frac{\lambda(T-\mu)^2}{2\mu^2 T}\right]$$

Quantum model: phase diffusion.

Additional notes on phase diffusion.

Assume Wald distribution:

$$P(T) = \sqrt{\frac{\lambda}{2\pi T^3}} \exp\left[-\frac{\lambda(T-\mu)^2}{2\mu^2 T}\right]$$

Wald characteristic function is

$$\begin{aligned}\Theta(\theta) &= \int_0^\infty dT e^{i\theta T} P(T) \\ &= \exp\left[\frac{\lambda}{\mu}\left(1-\sqrt{\frac{i2\mu^2\theta}{\lambda}}\right)\right]\end{aligned}$$

Quantum model: phase diffusion.

Additional notes on phase diffusion.

Quantum model: phase diffusion.

Additional notes on phase diffusion.

Thus

$$\int_0^\infty dT\ P(T)e^{-i\omega T(n-m)} = \exp\left[\frac{\lambda}{\mu}\left(1-\sqrt{\frac{i2\mu^2\omega(n-m)}{\lambda}}\right)\right]$$

Quantum model: phase diffusion.

Additional notes on phase diffusion.

Thus

$$\int_0^\infty dT\ P(T)e^{-i\omega T(n-m)} = \exp\left[\frac{\lambda}{\mu}\left(1-\sqrt{\frac{i2\mu^2\omega(n-m)}{\lambda}}\right)\right]$$

Recall the variance

$$\sigma = \frac{\mu^3}{\lambda}$$

and consider the limit $\lambda \to 0$ with $\mu\omega = 1$ constant

Quantum model: phase diffusion.

Additional notes on phase diffusion.

Thus

$$\int_0^\infty dT\ P(T)e^{-i\omega T(n-m)} = \exp\left[\frac{\lambda}{\mu}\left(1-\sqrt{\frac{i2\mu^2\omega(n-m)}{\lambda}}\right)\right]$$

Recall the variance

$$\sigma = \frac{\mu^3}{\lambda}$$

and consider the limit $\lambda \to 0$ with $\mu\omega = 1$ constant

$$|\langle n|\mathcal{E}(\rho)|m\rangle| = e^{-\sqrt{\gamma|n-m|}}|\langle n|\rho(0)|m\rangle|$$

where $\gamma = \mu^2/\sigma$.
No decay if $n = m$, otherwise decays rapidly as $|n - m|$ increases.

Quantum model: measurement noise

Writing $\rho_c(t)$ as a mixture of coherent states as

$$\rho_c(t) = \int d^2\alpha P_c(\alpha, t)|\alpha\rangle\langle\alpha|$$

define $\alpha = re^{i\phi}$

$$d\phi_c = \sqrt{\Gamma} dW$$

non-thermal phase diffusion rate $\Gamma = \kappa/2\bar{n}$.

From a laser to an atomic clock.

Add a counter.

From a laser to an atomic clock.

Add a counter.

Not easy for optical frequencies. Use mode-locking to produce a 'beat' signal at electronic frequencies so as to count.

From a laser to an atomic clock.

Add a counter.

Not easy for optical frequencies. Use mode-locking to produce a 'beat' signal at electronic frequencies so as to count.

All lasers are different due to technical noise.

From a laser to an atomic clock.

Add a counter.

Not easy for optical frequencies. Use mode-locking to produce a 'beat' signal at electronic frequencies so as to count.

All lasers are different due to technical noise.

Solution: All atoms are the same. Use measurement feedback to lock a laser to an atomic frequency.

Atomic clock.

An atomic clock consists of three distinct systems:

1. the "physics package," which produces atoms in the lower state of the clock transition;
2. the "electronics package," which generates the frequency needed to induce the transition in the reference atoms, which detects these transitions, and which then locks the frequency of the generator to the maximum of the transition rate,
3. the output system converts the frequency to one suitable for comparisons with other devices or for driving clock hardware.

Atomic clocks.

Ramsey interferometer .

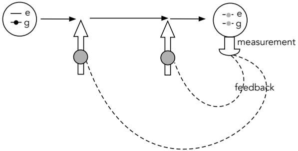

A single two-level atom is prepared in the ground state. It is then subjected to a $\pi/2$ pulse using a laser detuned by $\delta = \omega_a - \omega_L$ from the atomic transition frequency. It undergoes a period of free evolution before another $\pi/2$ pulse. It is then measured in the atomic basis with results $x = \pm 1$ with $1 \leftrightarrow e$ and $-1 \leftrightarrow g$.

Ramsey interferometer .

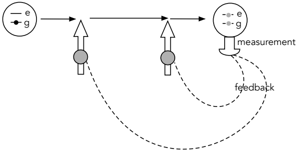

A single two-level atom is prepared in the ground state. It is then subjected to a $\pi/2$ pulse using a laser detuned by $\delta = \omega_a - \omega_L$ from the atomic transition frequency. It undergoes a period of free evolution before another $\pi/2$ pulse. It is then measured in the atomic basis with results $x = \pm 1$ with $1 \leftrightarrow e$ and $-1 \leftrightarrow g$.

ω_a fluctuates much less than ω_L.

Ramsey interferometer .

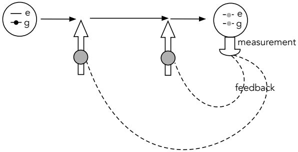

A single two-level atom is prepared in the ground state. It is then subjected to a $\pi/2$ pulse using a laser detuned by $\delta = \omega_a - \omega_L$ from the atomic transition frequency. It undergoes a period of free evolution before another $\pi/2$ pulse. It is then measured in the atomic basis with results $x = \pm 1$ with $1 \leftrightarrow e$ and $-1 \leftrightarrow g$.

ω_a fluctuates much less than ω_L.

A feedback control can be used to change the detuning for the next atom injected into the device with the goal of locking ω_L to the atomic transition frequency.

Ramsey interferometer .

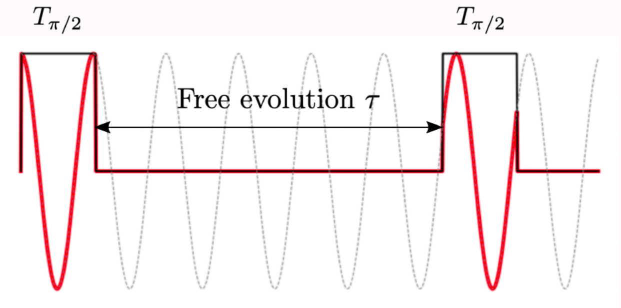

Ramsey interferometer.

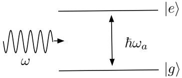

$$H = \frac{\hbar\omega_a}{2}\sigma_z + \hbar\Omega\cos(\omega_L t + \phi)\sigma_x$$

$\sigma_z = |e\rangle\langle e| - |g\rangle\langle g|$, $\sigma_x = |e\rangle\langle g| + |g\rangle\langle e|$,

Ramsey interferometer.

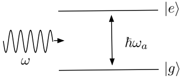

$$H = \frac{\hbar\omega_a}{2}\sigma_z + \hbar\Omega\cos(\omega_L t + \phi)\sigma_x$$

$\sigma_z = |e\rangle\langle e| - |g\rangle\langle g|$, $\sigma_x = |e\rangle\langle g| + |g\rangle\langle e|$, Initial state: $|\psi(0)\rangle = |g\rangle$
Evolve in interaction picture.

Ramsey interferometer.

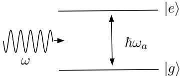

$$H = \frac{\hbar\omega_a}{2}\sigma_z + \hbar\Omega\cos(\omega_L t + \phi)\sigma_x$$

$\sigma_z = |e\rangle\langle e| - |g\rangle\langle g|$, $\sigma_x = |e\rangle\langle g| + |g\rangle\langle e|$, Initial state: $|\psi(0)\rangle = |g\rangle$
Evolve in interaction picture.

Probability to find system in excited state:

$$P_e(t) = \frac{\Omega^2}{\tilde{\Omega}^2}\sin^2\left[\frac{\tilde{\Omega}\ t}{2}\right]$$

$\tilde{\Omega} = \sqrt{\Omega^2 + \delta^2}$, $\delta = \omega_a - \omega_L$.

Ramsey interferometer.

Use a $\pi/2$ pulse such that $P_e(t) = 0.5$. Interaction time;

$$T = \frac{2}{\tilde{\Omega}} \sin^{-1}\left[\frac{\tilde{\Omega}}{\Omega\sqrt{2}}\right]$$

Ramsey interferometer.

Use a $\pi/2$ pulse such that $P_e(t) = 0.5$. Interaction time;

$$T = \frac{2}{\tilde{\Omega}} \sin^{-1}\left[\frac{\tilde{\Omega}}{\Omega\sqrt{2}}\right]$$

Then evolve freely for a time τ using the interaction picture Hamiltonian $H_0 = \frac{\hbar\delta}{2}\sigma_z$

Ramsey interferometer.

Use a $\pi/2$ pulse such that $P_e(t) = 0.5$. Interaction time;

$$T = \frac{2}{\tilde{\Omega}} \sin^{-1}\left[\frac{\tilde{\Omega}}{\Omega\sqrt{2}}\right]$$

Then evolve freely for a time τ using the interaction picture Hamiltonian $H_0 = \frac{\hbar\delta}{2}\sigma_z$

Followed by a second $\pi/2$ pulse. The total transformation,

$$U(\tau, T) = U_R(T)U_0(\tau)U_R(T)$$

where

$$U_R = \begin{pmatrix} \cos(A/2) + i\frac{\delta}{\tilde{\Omega}}sin(A/2) & -i\frac{\Omega|}{\tilde{\Omega}}\sin A/2 \\ -i\frac{\Omega|}{\tilde{\Omega}}\sin A/2 & \cos(A/2) - i\frac{\delta}{\tilde{\Omega}}\sin(A/2) \end{pmatrix}$$

$$U_0(\tau) = \begin{pmatrix} e^{i\delta t/2} & 0 \\ 0 & e^{-i\delta t/2} \end{pmatrix} \qquad A = \tilde{\Omega}T$$

Ramsey interferometer.

Probability to find in excited state

$$P_e = \cos^2\left(\frac{\delta\tau}{2} + \chi\right)$$

$\sin\chi = \delta/\Omega$.

Ramsey interferometer.

Probability to find in excited state

$$P_e = \cos^2\left(\frac{\delta\tau}{2} + \chi\right)$$

$\sin\chi = \delta/\Omega$. If second pulse has phase off-set ϕ

$$P_e = \cos^2\left(\frac{\delta\tau}{2} + \chi + \phi\right)$$

Ramsey interferometer.

$$\omega_a = 2\pi \times 1,\ \delta = 2\pi \times 0.2,\ \Omega = 2\pi \times 0.4$$

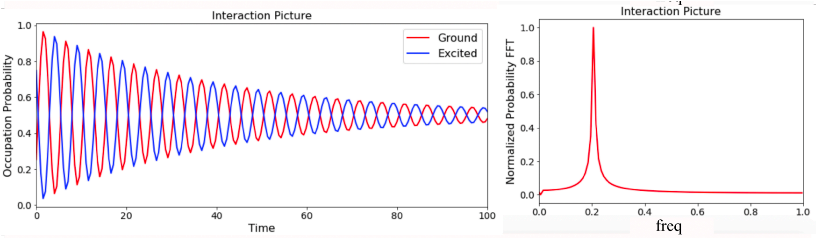

Avinash Rustagi

Ramsey interferometer.

Prior readout the atomic state is transformed:

$$|g\rangle \to U(\delta)|g\rangle = \cos(\delta\tau/2)|e\rangle + i\sin(\delta\tau/2)|g\rangle$$

assume χ is small.

Ramsey interferometer.

Prior readout the atomic state is transformed:

$$|g\rangle \rightarrow U(\delta)|g\rangle = \cos(\delta\tau/2)|e\rangle + i\sin(\delta\tau/2)|g\rangle$$

assume χ is small.
The measurement statistics:

$$\begin{aligned} p(x=+1|\delta) &= \cos^2(\delta\tau/2) \\ p(x=-1|\delta) &= \sin^2(\delta\tau/2) \end{aligned}$$

Operating point: $\delta\tau = \pi/2$, both measurement results are equally probable. At this point the slope of $p(x)$ versus $\delta\tau$

Ramsey interferometer.

Prior distribution for the detuning:

$$P(\delta) = \frac{1}{\sqrt{2\pi\sigma}}\; e^{-\frac{(\delta-\bar{\delta})^2}{2\sigma}}$$

where $\bar{\delta}\tau = \pi/2$.

Ramsey interferometer.

Prior distribution for the detuning:

$$P(\delta) = \frac{1}{\sqrt{2\pi\sigma}}\; e^{-\frac{(\delta-\bar{\delta})^2}{2\sigma}}$$

where $\bar{\delta}\tau = \pi/2$.
Conditioned on the measurement result, the a posteori distribution:

$$P(\delta|x) = \frac{P(\delta)p(x|\delta)}{p(x)} \qquad \text{(Baye's)}$$

where

$$p(x) = \int d\delta P(\delta)P(\delta|x)$$

Ramsey interferometer.

Prior distribution for the detuning:

$$P(\delta) = \frac{1}{\sqrt{2\pi\sigma}}\ e^{-\frac{(\delta-\bar{\delta})^2}{2\sigma}}$$

where $\bar{\delta}\tau = \pi/2$.

Conditioned on the measurement result, the a posteori distribution:

$$P(\delta|x) = \frac{P(\delta)p(x|\delta)}{p(x)} \qquad \text{(Baye's)}$$

where

$$p(x) = \int d\delta P(\delta)P(\delta|x)$$

$$\begin{aligned} P(\delta|+) &= 2\cos^2(\delta\tau/2)\frac{1}{\sqrt{2\pi\sigma}}\ e^{-\frac{(\delta-\bar{\delta})^2}{2\sigma}} \\ P(\delta|-) &= 2\sin^2(\delta\tau/2)\frac{1}{\sqrt{2\pi\sigma}}\ e^{-\frac{(\delta-\bar{\delta})^2}{2\sigma}} \end{aligned}$$

Ramsey interferometer.

Change of variable $z = \delta - \bar{\delta}$.

Conditional distribution after a long sequence of measurements. With $\bar{\delta}\tau = \pi/2$

$$p(x|z) = \frac{1}{2}(1 + x\sin(z\tau))$$

Thus

$$p(x) = \frac{1}{2}\int_{-\infty}^{\infty} dz P(z)(1 + x\sin(z\tau)) = 0.5$$

Ramsey interferometer.

Let $s_n = \{x_1, x_2, \ldots, x_n\}$ be a particular measurement history. This occurs with probability $p(s_n) = 2^{-n}$.

Ramsey interferometer.

Let $s_n = \{x_1, x_2, \ldots, x_n\}$ be a particular measurement history. This occurs with probability $p(s_n) = 2^{-n}$.

The conditional distribution

$$P(z|s_n) = \frac{\tilde{P}(z|s_n)}{p(s_n)}$$

$$\tilde{P}(z|s_n) = P(z) \prod_{k=1}^{n} p(x_k|z)$$

is the unnormalised conditional distribution.

Ramsey interferometer.

Let $s_n = \{x_1, x_2, \ldots, x_n\}$ be a particular measurement history. This occurs with probability $p(s_n) = 2^{-n}$.

The conditional distribution

$$P(z|s_n) = \frac{\tilde{P}(z|s_n)}{p(s_n)}$$

$$\tilde{P}(z|s_n) = P(z) \prod_{k=1}^{n} p(x_k|z)$$

is the unnormalised conditional distribution.

Thus

$$P(z|s_n) = P(z) \prod_{k=1}^{n} (1 + x_k \sin(z\tau))$$

Ramsey interferometer.

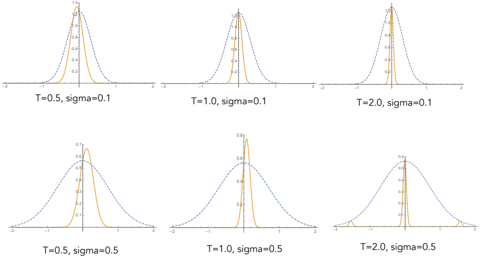

Conditional (unnormalised) distribution for the detuning conditioned on the results of $n = 10$ random histories for different values of σ and τ.

Ramsey interferometer.

The feedback protocol changes the distribution for the detuning, conditioned on the measurement result, prior to the next atom entering the apparatus.

$$P(z|x) \to P(z - \epsilon x|x)$$

assumes no added noise in feedback loop.

Ramsey interferometer.

The feedback protocol changes the distribution for the detuning, conditioned on the measurement result, prior to the next atom entering the apparatus.

$$P(z|x) \to P(z - \epsilon x|x)$$

assumes no added noise in feedback loop.
unconditional detuning distribution after the feedback.

$$P'(z) = P(z + \epsilon|+)p(+) + P(z - \epsilon|-)p(-)$$

We can compute the change in variance

$$V' = V - \epsilon\sigma\tau e^{-\sigma\tau^2/2} + \epsilon^2$$

Ramsey interferometer.

minimize over ϵ and τ. This gives the optimal values,

$$\tau_{opt} = \frac{1}{\sqrt{\sigma}}$$
$$\epsilon_{opt} = \sqrt{\frac{\sigma}{4e}}$$

$$V' = \sigma(1 - \frac{1}{4e}) \approx 0.9\sigma$$

using $V(z) = \sigma$.

Iterated over many cycles we find that the variance in the detuning distribution can be made arbitrarily small.

need σ small so τ needs to be large.

In reality, feedback loop is not noise-free.

Cs atomic fountain clock.

MOT

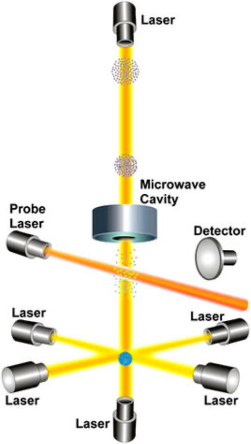

Cs atomic fountain clock.

$\tau =$ time of free flight over about one metre ... about 10ms.

Cs atomic fountain clock.

$\tau =$ time of free flight over about one metre ... about 10ms.

Need interaction time in the cavity to be well defined to get a $\pi/2$ pulse.

Cs atomic fountain clock.

$\tau =$ time of free flight over about one metre ... about 10ms.

Need interaction time in the cavity to be well defined to get a $\pi/2$ pulse.

Need well-defined velocity ... cooling.. about 100m/s

Cs atomic fountain clock.

$\tau =$ time of free flight over about one metre ... about 10ms.

Need interaction time in the cavity to be well defined to get a $\pi/2$ pulse.

Need well-defined velocity ... cooling.. about 100m/s

Microwave is driven and locked to a cryogenic sapphire clock.

Cs atomic fountain clock.

Level structure:

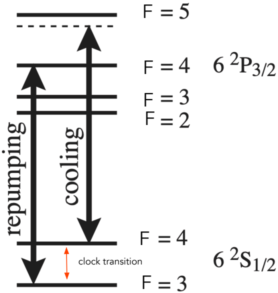

Cooling laser tuned to the red of the $F = 4 \rightarrow F = 5$ transition .

Clock transition frequency defined as 9.19263177 GHz.

Cs atomic fountain clock:readout

Readout is done by the method of fluorescence cycling.

Cs atomic fountain clock:readout

Readout is done by the method of fluorescence cycling.

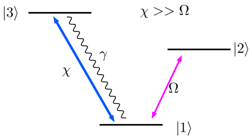

Cs atomic fountain clock:readout

Readout is done by the method of fluorescence cycling.

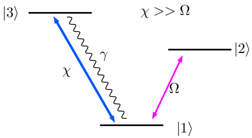

Adiabatically eliminate level-3.

$$\rho_{33} \approx \frac{\chi^2}{\gamma^2}\rho_{11}$$

Cs atomic fountain clock:readout

Readout is done by the method of fluorescence cycling.

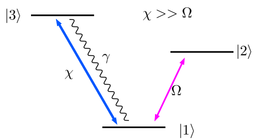

Adiabatically eliminate level-3.

$$\rho_{33} \approx \frac{\chi^2}{\gamma^2}\rho_{11}$$

Fluorescence intensity

$$I_{fl} \propto \gamma\rho_{33} \approx \frac{\chi^2}{\gamma}\rho_{11}$$

determined by population in level-1.

Cs atomic fountain clock:readout

Effective master equation for the $1-2$ subsystem

$$\dot{\rho} = -i\frac{\Omega}{2}[\sigma_x, \rho] - \Gamma[\sigma_z[\sigma_z, \rho]]$$

$\sigma_x = |2\rangle\langle 1| + |1\rangle\langle 2|, \ \sigma_z = |2\rangle\langle 2| - |1\rangle\langle 1|$

$$\Gamma = \frac{\chi^2}{2\gamma}$$

Cs atomic fountain clock:readout

Effective master equation for the $1-2$ subsystem

$$\dot{\rho} = -i\frac{\Omega}{2}[\sigma_x, \rho] - \Gamma[\sigma_z[\sigma_z, \rho]]$$

$\sigma_x = |2\rangle\langle 1| + |1\rangle\langle 2|, \ \sigma_z = |2\rangle\langle 2| - |1\rangle\langle 1|$

$$\Gamma = \frac{\chi^2}{2\gamma}$$

Rapid diagonalisation in eigenstates for $\Gamma >> 1$. Large fluorescent intensity.

Cs atomic fountain clock:readout

Effective master equation for the $1-2$ subsystem

$$\dot{\rho} = -i\frac{\Omega}{2}[\sigma_x, \rho] - \Gamma[\sigma_z[\sigma_z, \rho]]$$

$\sigma_x = |2\rangle\langle 1| + |1\rangle\langle 2|, \ \sigma_z = |2\rangle\langle 2| - |1\rangle\langle 1|$

$$\Gamma = \frac{\chi^2}{2\gamma}$$

Rapid diagonalisation in eigenstates for $\Gamma >> 1$. Large fluorescent intensity.

Γ is the measurement rate.

Cs atomic fountain clock:readout

Integrate fluorescent intensity

$$N_3 \propto \int dt I_{fl}(t)$$

Cs atomic fountain clock:readout

Integrate fluorescent intensity

$$N_3 \propto \int dt I_{fl}(t)$$

In atomic fountain experiment both $F = 3$ and $F = 4$ are readout by a fluorescent signal.

Cs atomic fountain clock:readout

Integrate fluorescent intensity

$$N_3 \propto \int dt I_{fl}(t)$$

In atomic fountain experiment both $F = 3$ and $F = 4$ are readout by a fluorescent signal.
In the servo system the ratio $N = N_4/(N_3 + N_4)$ is calculated.

This ratio is independent of the shot-to- shot fluctuations in atom number, which typically lie in the percent range, and is used as the input signal to the microwave-frequency servo loop.

Cs atomic fountain clock: noise.

quantum projection noise:

Cs atomic fountain clock: noise.

quantum projection noise:

Recall

$$
\begin{aligned}
p(x=+1|\delta) &= \cos^2(\delta\tau/2) \equiv p_+ \\
p(x=-1|\delta) &= \sin^2(\delta\tau/2) \equiv p_-
\end{aligned}
$$

Cs atomic fountain clock: noise.

quantum projection noise:

Recall

$$\begin{aligned} p(x=+1|\delta) &= \cos^2(\delta\tau/2) \equiv p_+ \\ p(x=-1|\delta) &= \sin^2(\delta\tau/2) \equiv p_- \end{aligned}$$

mean: $\bar{x} = p_+ - p_- = 2p_+ - 1 = \cos(\delta\tau)$

variance: $\overline{\Delta x^2} = 4p_+(1-p_+)$ ... projection noise.

Cs atomic fountain clock: noise.

N atoms:

$$y = \frac{1}{N}\sum_{j=1}^{n} x_j$$

a random variable.

Cs atomic fountain clock: noise.

N atoms:

$$y = \frac{1}{N}\sum_{j=1}^{n} x_j$$

a random variable.

Law of large numbers:
mean $\bar{y} = 2p_+ - 1 = \cos(\delta\tau)$

variance $\overline{\Delta y^2} = \frac{4p_+(1-p_+)}{N} = \frac{sin(\delta\tau)^2}{N}$

Cs atomic fountain clock: noise.

N atoms:

$$y = \frac{1}{N}\sum_{j=1}^{n} x_j$$

a random variable.

Law of large numbers:
mean $\bar{y} = 2p_+ - 1 = \cos(\delta\tau)$

variance $\overline{\Delta y^2} = \frac{4p_+(1-p_+)}{N} = \frac{sin(\delta\tau)^2}{N}$

Fractional error to estimate δ

$$\sigma = \frac{\sqrt{\overline{\Delta y^2}}}{\left|\frac{\partial\bar{y}}{\partial\delta}\right|} = \frac{1}{\tau\sqrt{N}}$$

Cs atomic fountain clock: noise.

Other sources of noise:

1. Poisson distributed photon number fluctuations in the detected intensity of the fluorescence.
2. electronic detection noise in detection circuit. DOMINANT.
3. Finite decay time of the clock transition.
4. Phase noise in the microwave field (Dicke effect).

1 dominates.

Cs atomic fountain clock: noise.

Cs atomic fountain clock: noise.

While all Cs atoms are the same, they experience different environments and have frequency off-sets that depend on the experiment.

- stray electric and magnetic fields
- Doppler effects
- atomic collisions
- gravitational effects

Cs atomic fountain clock: noise.

While all Cs atoms are the same, they experience different environments and have frequency off-sets that depend on the experiment.

- stray electric and magnetic fields
- Doppler effects
- atomic collisions
- gravitational effects

All clocks depend on the local environment.

Cs atomic fountain clock: noise.

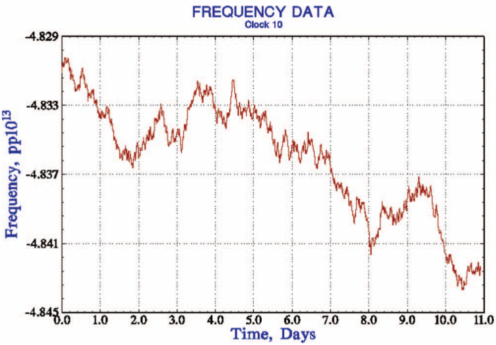

FIG. 1. (Color online) The frequency of a cesium frequency standard with respect to the NIST clock ensemble.

Levin 2012

Linear sensors.

Quantum parameter estimation.

Linear sensors.

Optical accelerometer: The parameter of interest is an acceleration in the horizontal direction. What is measured is the displacement of the proof mass due to this acceleration. The optical measurement scheme seeks to detect the change in the relative arm length and estimate the acceleration.

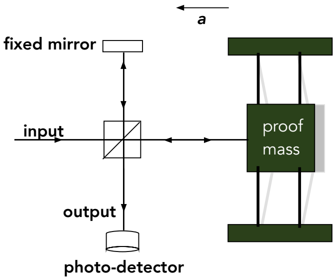

Linear sensors.

The spring constant: k, Proof mass: m_0.

Linear sensors.

The spring constant: k, Proof mass: m_0.

Displacement from equilibrium is $x =$ change in the relative path length for the interferometer.

Linear sensors.

The spring constant: k, Proof mass: m_0.

Displacement from equilibrium is $x =$ change in the relative path length for the interferometer.

Time-dependent force $f(t) = m_0 a(t)$

Linear sensors.

The spring constant: k, Proof mass: m_0.

Displacement from equilibrium is $x =$ change in the relative path length for the interferometer.

Time-dependent force $f(t) = m_0 a(t)$

Assume the oscillator is heavily damped with damping rate η and that the temperature of the environment is T. Langevin equaiton:

$$\frac{dx}{dt} = -\frac{\omega_0^2}{\gamma}x + (a/\gamma)dt + \sigma\xi(t)$$

where the fluctuation-dissipation theorem requires that $\sigma^2 = 2k_B T\gamma$.

Linear sensors.

The stationary solution for the displacement is

$$\mathrm{P}(x|a) = e^{-(x-a/\omega_0^2)^2/2\Delta}$$

Linear sensors.

The stationary solution for the displacement is

$$\mathrm{P}(x|a) = e^{-(x-a/\omega_0^2)^2/2\Delta}$$

The mean and variance of the displacement is

$$\bar{x} = \frac{a}{\omega_0^2}, \quad \Delta = \frac{k_B T}{m_0 \omega_0^2}$$

Linear sensors.

The stationary solution for the displacement is

$$\mathrm{P}(x|a) = e^{-(x-a/\omega_0^2)^2/2\Delta}$$

The mean and variance of the displacement is

$$\bar{x} = \frac{a}{\omega_0^2}, \quad \Delta = \frac{k_B T}{m_0 \omega_0^2}$$

In order to estimate a we need to measure the displacement and form the empirical average

$$a_{est} = \omega_0^2 \frac{1}{N} \sum_{n=1}^{N} x_n$$

The deviation of the estimate from the parameter is $\delta a = a_{est} - a$.

Linear sensors.

The precision of the estimation is the second moment of δa. This is bounded below by the Cramer-Rao lower bound:

$$\mathbb{E}[(\delta a)^2] \geq \frac{1}{NF(a)}$$

where $F(a)$ is the Fisher information defined by

$$F(a) \equiv \int dx \frac{1}{P(x|a)} \left(\frac{\partial P(x|a)}{\partial a} \right)^2$$

Linear sensors.

The precision of the estimation is the second moment of δa. This is bounded below by the Cramer-Rao lower bound:

$$\mathbb{E}[(\delta a)^2] \geq \frac{1}{NF(a)}$$

where $F(a)$ is the Fisher information defined by

$$F(a) \equiv \int dx \frac{1}{P(x|a)} \left(\frac{\partial P(x|a)}{\partial a} \right)^2$$

In this case $F(a) = \Delta$ so the precision is bounded by

$$\mathbb{E}[(\delta a)^2] \geq \frac{k_B T}{N m_0 \omega_0^2}$$

This scheme constitutes a linear sensor as $\bar{x} \propto a$.

Linear sensors.

The precision of the estimation is the second moment of δa. This is bounded below by the Cramer-Rao lower bound:

$$\mathbb{E}[(\delta a)^2] \geq \frac{1}{NF(a)}$$

where $F(a)$ is the Fisher information defined by

$$F(a) \equiv \int dx \frac{1}{P(x|a)} \left(\frac{\partial P(x|a)}{\partial a} \right)^2$$

In this case $F(a) = \Delta$ so the precision is bounded by

$$\mathbb{E}[(\delta a)^2] \geq \frac{k_B T}{N m_0 \omega_0^2}$$

This scheme constitutes a linear sensor as $\bar{x} \propto a$.

The estimate can be improved by lowering the temperature, or increasing the mass or increasing the oscillator frequency.

Quantum metrology.

Quantum parameter estimation:

See Braunstein et al. Annals of physics (1996).

Quantum parameter estimation.

One parameter unitary transformations

$$\rho_0 \to \rho_\theta = e^{-i\theta\hat{G}}\rho e^{i\theta\hat{G}}.$$

Quantum parameter estimation.

One parameter unitary transformations

$$\rho_0 \to \rho_\theta = e^{-i\theta\hat{G}}\rho e^{i\theta\hat{G}}.$$

Generalized measurement: $E(\xi)$, result ξ, and $\int d\xi E(\xi) = I_d$.

$$p(\xi|\theta) = \mathrm{tr}(E(\xi)\rho(\theta))$$

.

Quantum parameter estimation.

One parameter unitary transformations

$$\rho_0 \to \rho_\theta = e^{-i\theta\hat{G}}\rho e^{i\theta\hat{G}}.$$

Generalized measurement: $E(\xi)$, result ξ, and $\int d\xi E(\xi) = I_d$.

$$p(\xi|\theta) = \mathrm{tr}(E(\xi)\rho(\theta))$$

.

N independent trials θ, estimate $\theta_{est} = \theta_{est}(\xi_1, \xi_2, ..., \xi_N)$

Quantum parameter estimation.

One parameter unitary transformations

$$\rho_0 \to \rho_\theta = e^{-i\theta\hat{G}}\rho e^{i\theta\hat{G}}.$$

Generalized measurement: $E(\xi)$, result ξ, and $\int d\xi E(\xi) = I_d$.

$$p(\xi|\theta) = \mathrm{tr}(E(\xi)\rho(\theta))$$

.

N independent trials θ, estimate $\theta_{est} = \theta_{est}(\xi_1, \xi_2, ..., \xi_N)$

deviation of estimate from the actual value:

$$\delta\theta \equiv \theta_{est} - \theta$$

Quantum parameter estimation.

Find a lower bound to the mean square deviation of the estimate

Quantum parameter estimation.

Find a lower bound to the mean square deviation of the estimate

Cramér-Rao bound:

$$\langle(\delta\theta)^2\rangle \geq \frac{1}{NF(\theta)}$$

where N is the number of measurement results used in the estimation, and $F(\theta)$, Fisher information:

$$\begin{aligned} F(\theta) &\equiv \int d\xi p(\xi|\theta)\left(\frac{\partial \ln p(\xi|\theta)}{\partial\theta}\right)^2 \\ &= \int d\xi \frac{1}{p(\xi|\theta)}\left(\frac{\partial p(\xi|\theta)}{\partial\theta}\right)^2 \end{aligned}$$

Quantum parameter estimation.

Braunstein & Caves, PRL (1004). Optimise over all POVMs

$$\max_{\rho_0} \max_{\{E(\xi)\}} F(\theta)$$

Quantum parameter estimation.

Braunstein & Caves, PRL (1004). Optimise over all POVMs

$$\max_{\rho_0} \max_{\{E(\xi)\}} F(\theta)$$

For

$$\rho_\theta = e^{-i\theta\hat{G}}\rho e^{i\theta\hat{G}}.$$

$$\langle(\delta\theta)^2\rangle \geq \frac{1}{\langle\Delta\hat{G}^2\rangle}$$

where $\langle\Delta\hat{G}^2\rangle$ is the variance for $\hat{G}$ in fiducial state $\rho(0)$.

Quantum parameter estimation.

Example: estimating displacements.

Quantum parameter estimation.

Example: estimating displacements. Momentum is the generator of displacements:

$$\rho(x) = e^{-ix\hat{p}/\hbar}\rho(0)e^{ix\hat{p}/\hbar}$$

As

$$e^{ix\hat{p}/\hbar}\hat{q}e^{-ix\hat{p}/\hbar} = \hat{q} + x$$

Quantum parameter estimation.

Example: estimating displacements. Momentum is the generator of displacements:

$$\rho(x) = e^{-ix\hat{p}/\hbar}\rho(0)e^{ix\hat{p}/\hbar}$$

As

$$e^{ix\hat{p}/\hbar}\hat{q}e^{-ix\hat{p}/\hbar} = \hat{q} + x$$

$$\delta x \geq \frac{1}{\sqrt{N\langle\Delta\hat{p}^2\rangle}}$$

Do not confuse with HUP!

Quantum parameter estimation.

What is the fiducial state?

Quantum parameter estimation.

What is the fiducial state?

Example: quantum ruler: superposition of momentum eigenstates.

$$|\psi_0\rangle \sim |p_0\rangle + |-p_0\rangle$$

Note this is not a physical state.

Quantum parameter estimation.

What is the fiducial state?

Example: quantum ruler: superposition of momentum eigenstates.

$$|\psi_0\rangle \sim |p_0\rangle + |-p_0\rangle$$

Note this is not a physical state. Position probability density

$$P(x|p_0) \sim |e^{-ip_0x/\hbar} + e^{ip_0x/\hbar}|^2 \sim \cos(p_0x/\hbar)^2$$

fringe spacing $\delta x \sim 1/p_0$.

Quantum parameter estimation.

What is the fiducial state?

Example: quantum ruler: superposition of momentum eigenstates.

$$|\psi_0\rangle \sim |p_0\rangle + |-p_0\rangle$$

Note this is not a physical state. Position probability density

$$P(x|p_0) \sim |e^{-ip_0 x/\hbar} + e^{ip_0 x/\hbar}|^2 \sim \cos(p_0 x/\hbar)^2$$

fringe spacing $\delta x \sim 1/p_0$.

Variance in momentum

$$\langle \Delta \hat{p}^2 \rangle \sim (p_0)^2$$

Maximise variance in momentum maximises fringe spacing.

Quantum parameter estimation.

Repeat N times

$$\delta x \geq \frac{1}{\sqrt{N} p_0} \qquad \text{Standard quanutm limit (SQL)}$$

Requires a product state of N particles.

Quantum parameter estimation.

Repeat N times

$$\delta x \geq \frac{1}{\sqrt{N} p_0} \qquad \text{Standard quanutm limit (SQL)}$$

Requires a product state of N particles.

Can we do better if we entangle all N particles first?

$$|\psi_0\rangle \sim |p_0, p_0, \ldots p_0\rangle + |-p_0, -p_0, \ldots - p_0\rangle$$

Quantum parameter estimation.

Repeat N times

$$\delta x \geq \frac{1}{\sqrt{N} p_0} \qquad \text{Standard quanutm limit (SQL)}$$

Requires a product state of N particles.

Can we do better if we entangle all N particles first?

$$|\psi_0\rangle \sim |p_0, p_0, \ldots p_0\rangle + |-p_0, -p_0, \ldots - p_0\rangle$$

Position probability density

$$P_N(x|p_0) \sim |e^{-ip_0 x/\hbar} + e^{ip_0 x/\hbar}|^{2N} \sim \cos(p_0 x/\hbar)^{2N}$$

Quantum parameter estimation.

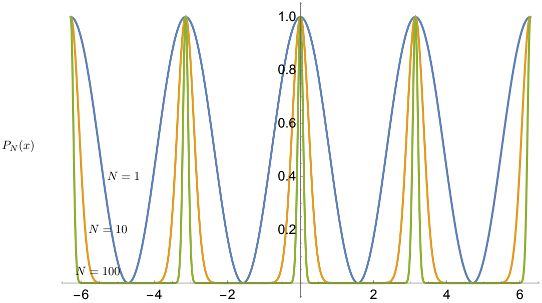

Quantum parameter estimation.

Define collective momentum operator

$$\hat{P} = \sum_{j=1}^{N} \hat{p}_j$$

Find

$$Var(\hat{P}) = N^2 p_0^2$$

So

$$\delta x \geq \frac{1}{N p_0}$$

improved by a factor of $1/\sqrt{N}$

Quantum sensing.

Quantum coherence is very sensitive to interactions with the environment (decherence).

Quantum sensing.

Quantum coherence is very sensitive to interactions with the environment (decherence).

Bad for quantum computers.

Quantum sensing.

Quantum coherence is very sensitive to interactions with the environment (decherence).

Bad for quantum computers.

Great for quantum sensing!

Quantum sensing.

Quantum coherence is very sensitive to interactions with the environment (decherence).

Bad for quantum computers.

Great for quantum sensing!

Examples:

- Quantum magnetic sensors for brain imaging.
- Quantum gravimeters for underground voids and water levels.
- Quantum inertial sensors for navigation.
- Quantum clocks for back-up under GPS denial.

Magnetic field sensing with NV diamond.

The NV centre is a point defect in diamond consisting of a substitutional nitrogen with a vacancy in its nearest neighbour lattice site.

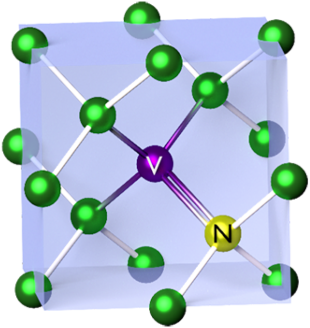

Magnetic field sensing with NV diamond.

The negatively charged state forms a spin triplet in the orbital ground state.

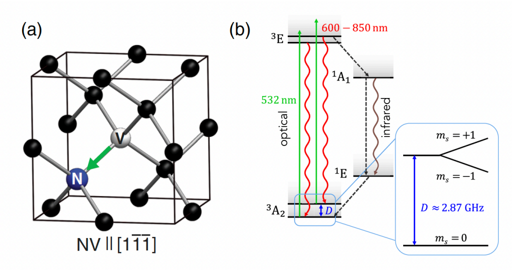

Magnetic field sensing with NV diamond.

The negatively charged state forms a spin triplet in the orbital ground state.

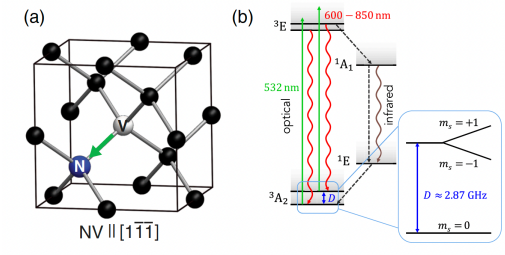

The crystal field splits these spin levels, resulting in the $m_s = 0$ state in the lowest energy state, and the $m_s = \pm 1$ sublevels lifted by 2.87 GHz.

Magnetic field sensing with NV diamond.

The negatively charged state forms a spin triplet in the orbital ground state.

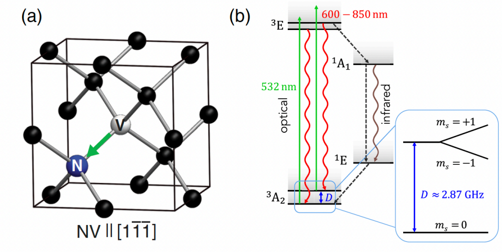

The crystal field splits these spin levels, resulting in the $m_s = 0$ state in the lowest energy state, and the $m_s = \pm 1$ sublevels lifted by 2.87 GHz.

Weak DC external magnetic field: $m_s = \pm 1$ have an energy splitting.

Magnetic field sensing with NV diamond.

The negatively charged state forms a spin triplet in the orbital ground state.

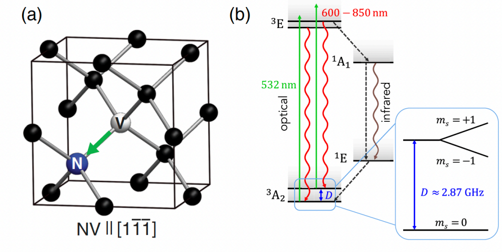

The crystal field splits these spin levels, resulting in the $m_s = 0$ state in the lowest energy state, and the $m_s = \pm 1$ sublevels lifted by 2.87 GHz.

Weak DC external magnetic field: $m_s = \pm 1$ have an energy splitting.

Weak AC external magnetic field: induces transitions between $m_s = 0$ and $m_s = \pm 1$.

Magnetic field sensing with NV diamond.

Optically Detected ESR/ODMR electron spin resonance.

Principle: ODMR leverages the spin-dependent fluorescence of NV centers. The NV center has a ground state and an excited state, both of which are spin triplets. When the NV center is optically excited, it can relax back to the ground state either directly or via a metastable singlet state. This relaxation process is spin-dependent, leading to varying fluorescence intensities depending on the spin state.

Relaxation to the $m_s = 0$ state results in a decrease in **visible** wavelength fluorescence (as the emitted photon is in the infrared range).

Magnetic field sensing with NV diamond.

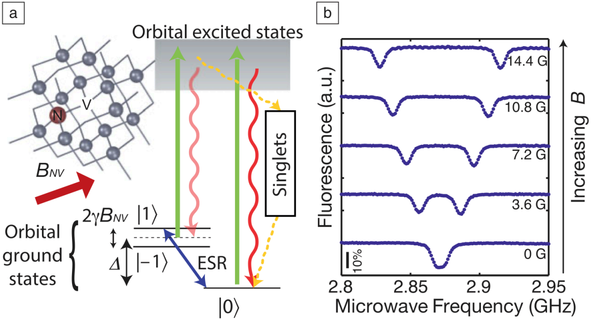

Figure 1. (a) Level diagram of a single nitrogen-vacancy (NV) center in diamond. A NV center emits fluorescence (red) under off-resonant optical excitation (green). When the NV center's spin state is $m_s = 1$ or -1, once optically excited, it decays through metastable singlet states to $m_s = 0$. This leads to optical initialization and spin-dependent fluorescence, which can be used to read out the probability of the spin state. ESR, electron spin resonance. (b) Optically detected ESR spectra as a function of magnetic field along the NV axis. The NV's spin triplet has a zero magnetic field splitting (Δ ~2.87 GHz), and $m_s = 1$ and -1 states are degenerate, resulting in a single spin resonance frequency. In an external field, $m_s = 1$ and -1 states split proportional to the field projected along the N–V axis, resulting in two spin resonance frequencies.

Hong et al. DOI: 10.1557/mrs.2013.23

Magnetic field sensing with NV diamond.

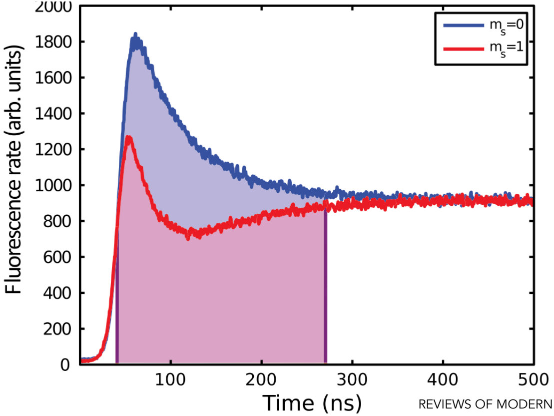

REVIEWS OF MODERN PHYSICS, VOLUME 92, JANUARY–MARCH 2020

FIG. 6. Fluorescence of the NV^- spin states. NV^- centers prepared in the $m_s = 0$ state emit photons at a higher rate than centers prepared in the $m_s = \pm 1$ states. This spin-dependent fluorescence forms the basis of conventional NV^- readout. Data courtesy of Brendan Shields.

Magnetic field sensing with NV diamond.

DC B sensing with Ramsey interferometry with ESR pulses.

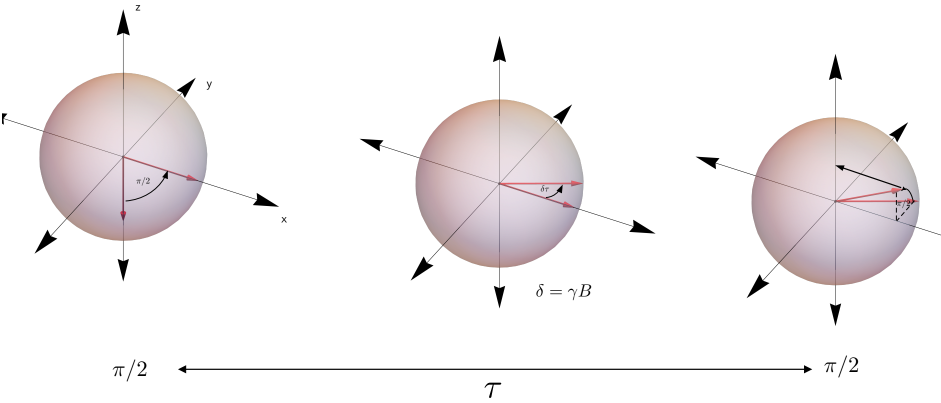

γ is gyromagnetic ratio of electron.

Magnetic field sensing with NV diamond.

State is $\cos(\gamma B\tau/2)|\uparrow\rangle + i\sin(\gamma B\tau/2)|\downarrow\rangle$

Readout $z-$ component via fluorescence.

Magnetic field sensing with NV diamond.

State is $\cos(\gamma B\tau/2)|\uparrow\rangle + i\sin(\gamma B\tau/2)|\downarrow\rangle$

Readout $z-$ component via fluorescence.

$$\begin{aligned} p(\uparrow|B) &= \cos^2(\gamma B\tau/2) \\ p(\downarrow|B) &= \sin^2(\gamma B\tau/2) \end{aligned}$$

Use this distribution to estimate B

Magnetic field sensing with NV diamond.

State is $\cos(\gamma B\tau/2)|\uparrow\rangle + i\sin(\gamma B\tau/2)|\downarrow\rangle$

Readout $z-$ component via fluorescence.

$$
\begin{aligned}
p(\uparrow|B) &= \cos^2(\gamma B\tau/2) \\
p(\downarrow|B) &= \sin^2(\gamma B\tau/2)
\end{aligned}
$$

Use this distribution to estimate B

$$\delta B \geq \frac{1}{\gamma\tau\sqrt{N}}$$

Magnetic field sensing with NV diamond.

State is $\cos(\gamma B\tau/2)|\uparrow\rangle + i\sin(\gamma B\tau/2)|\downarrow\rangle$

Readout $z-$ component via fluorescence.

$$\begin{aligned} p(\uparrow|B) &= \cos^2(\gamma B\tau/2) \\ p(\downarrow|B) &= \sin^2(\gamma B\tau/2) \end{aligned}$$

Use this distribution to estimate B

$$\delta B \geq \frac{1}{\gamma\tau\sqrt{N}}$$

We have ignored dephasing due to surrounding spins in the solid. The main source of electron spin decoherence is the nuclear spin bath arising from the presence of ^{13}C atoms

Magnetic field sensing with NV diamond.

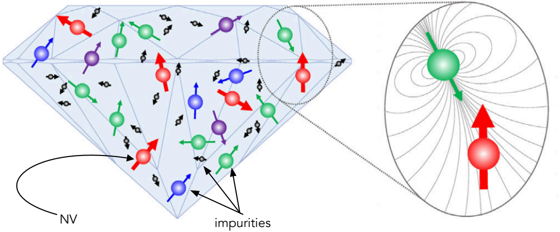

REVIEWS OF MODERN PHYSICS, VOLUME 92, JANUARY–MARCH 2020

Magnetic field sensing with NV diamond.

Hahn echo.

Ensemble of spins with inhomogeneous local B field

$$H = \frac{\hbar\omega}{2}\sigma_z + \frac{\hbar}{2}\sum_n \delta_n \sigma_z$$

Hahn-echo pulse sequence can improve the magnetic field sensitivity, provided that it measures an AC magnetic field with its period matched to the total free evolution time.

Magnetic field sensing with NV diamond.

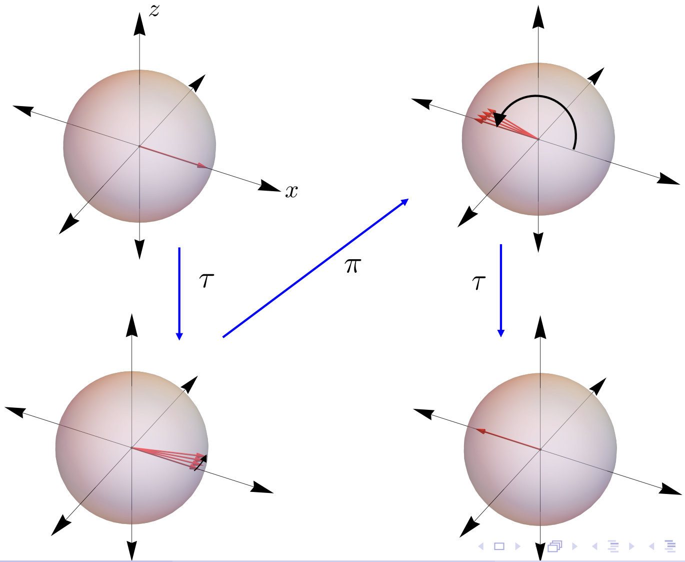

Magnetic field sensing with NV diamond.

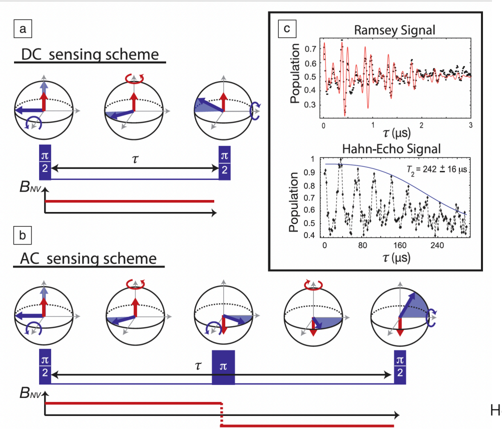

Hong et al. DOI: 10.1557/mrs.2013.23

Magnetic field sensing with NV diamond.

State-of-the-art ensemble ($N > 10^4$) NV magnetometers exhibit pT/$\sqrt{\text{Hz}}$-level sensitivities.

Can have atomic scale resolution in scanning.

DeVience,. et al. Nanoscale NMR spectroscopy and imaging of multiple nuclear species. Nature Nanotech 2015).
https://doi.org/10.1038/nnano.2014.313

Magnetic field sensing with NV diamond.

Kuwahata, A., Kitaizumi, T., Saichi, K. et al. Magnetometer with nitrogen-vacancy center in a bulk diamond for detecting magnetic nanoparticles in biomedical applications. Sci Rep 10, 2483 (2020). https://doi.org/10.1038/s41598-020-59064-6

Atomic sensor for electric fields .

Optical dipole transitions in a two-level system

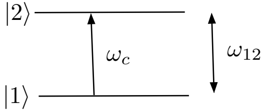

$$|\psi(t) = \cos(\Omega t/2)|1\rangle + i\sin(\Omega t/2)|2\rangle$$

Rabi frequency:

$$\Omega = \mu_{12}\tilde{E}/\hbar,$$

where $\tilde{E}$ is the electric field at the atomic position.

Atomic sensor for electric fields .

Rabi frequencies:

$$\Omega_{\mathrm{p}} = \mu_{13}\tilde{E}_1/\hbar, \quad \Omega_{\mathrm{c}} = \mu_{23}\tilde{E}_2/\hbar$$

$$\omega_p = \omega_{12} + \delta$$
$$\omega_c = \omega_{23} - \delta$$

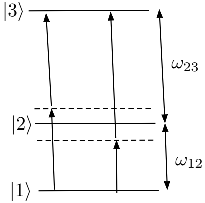

$$\omega_p = \omega_{12} - \delta$$
$$\omega_c = \omega_{23} + \delta$$

$$\Omega_p + \Omega_c = \omega_{12} + \omega_{23}$$

$\delta = 0 \rightarrow$ dark state $\quad |D\rangle = \left(\Omega_{\mathrm{p}}|2\rangle - \Omega_{\mathrm{c}}|1\rangle\right)/\Omega, \qquad \Omega = \sqrt{\Omega_p^2 + \Omega_c^2}$

This antisymmetric superposition of states $|1\rangle, |2\rangle$ has a zero transition rate to the excited state.

Atomic sensor for electric fields .

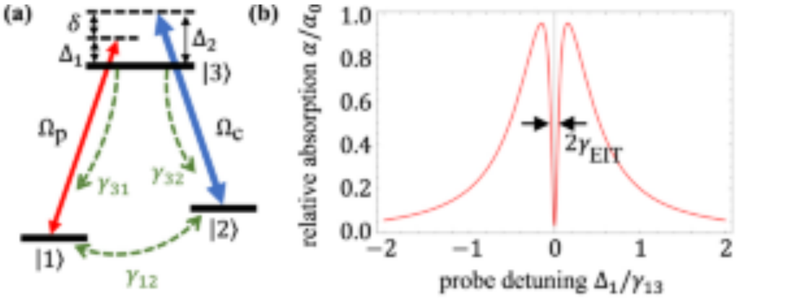

very narrow transparency window. : Electromagnetically induced transparency (EIT)

Atomic sensor for electric fields .

Rydberg Atoms and EIT: Rydberg atoms have one or more electrons in a highly excited state, which makes them extremely sensitive to external electric fields due to their large polarizability. EIT is used in these systems to create a transparency window in an otherwise opaque medium, allowing for precise measurements of field-induced shifts in energy levels.

Atomic sensor for electric fields .

Rydberg Atoms and EIT: Rydberg atoms have one or more electrons in a highly excited state, which makes them extremely sensitive to external electric fields due to their large polarizability. EIT is used in these systems to create a transparency window in an otherwise opaque medium, allowing for precise measurements of field-induced shifts in energy levels.

Stark Effect: The presence of a static electric field causes a shift in the energy levels of the Rydberg atoms, known as the Stark effect. By using EIT, one can measure these shifts with high precision. The EIT signal is sensitive to changes in the energy levels, and thus, changes in the electric field can be detected by monitoring the EIT transmission spectrum

Atomic sensor for electric fields .

Measurement Process: In a typical setup, a probe laser is used to excite the atoms to an intermediate state, while a coupling laser further excites them to a Rydberg state. The presence of a static electric field modifies the energy levels of the Rydberg state, which in turn affects the EIT signal. By analyzing the changes in the EIT spectrum, the magnitude and direction of the static electric field can be determined.

Atomic sensor for electric fields .

Measurement Process: In a typical setup, a probe laser is used to excite the atoms to an intermediate state, while a coupling laser further excites them to a Rydberg state. The presence of a static electric field modifies the energy levels of the Rydberg state, which in turn affects the EIT signal. By analyzing the changes in the EIT spectrum, the magnitude and direction of the static electric field can be determined.

Applications: This method is particularly useful for applications requiring high precision and sensitivity, such as voltage standards and electrometry. The ability to detect static fields with high accuracy makes Rydberg atom-based sensors valuable for various scientific and industrial applications.

Atomic sensor for electric fields .

Applications: Holloway, et al., Electromagnetically induced transparency based Rydberg-atom sensor for traceable voltage measurements. AVS Quantum Sci. 1 September 2022; 4 (3): 034401.
https://doi.org/10.1116/5.0097746

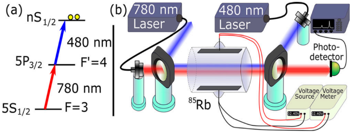

FIG. 2. (a) Level diagram depicting EIT coupling the $5S_{1/2}(F=3)$ state to an $nS_{1/2}(F=3)$ Rydberg state through the $5P_{3/2}(F=4)$ intermediate state. (b) Experimental setup for the voltage measurement and the three-level EIT scheme.

"State-of-the-art method for realizing the volt, the Josephson voltage standard, is significantly more accurate, the Rydberg atom-based method presented here has the potential to be a calibration standard with more favorable size, weight, power, and cost."

Atom sensors

Atom interferometers.

Stimulated Raman transitions.

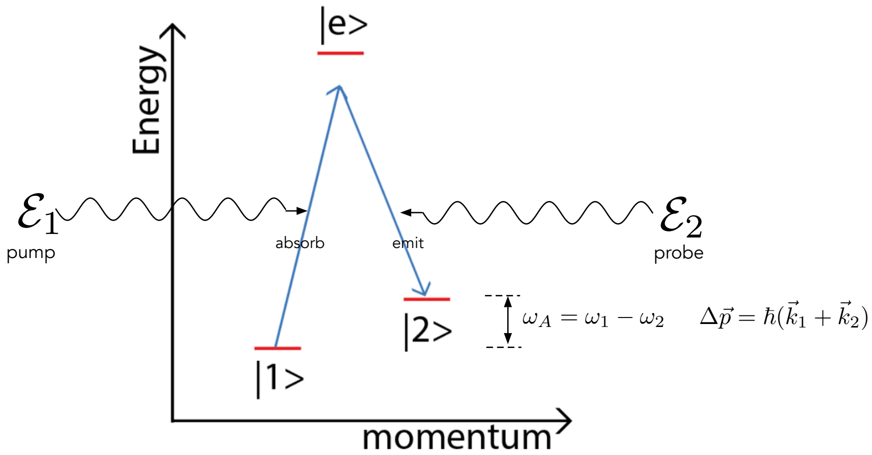

Atom interferometers.

Quantise centre-of-mass motion in $z-$ direction:

$$H = \hbar g \left[\mathcal{E}_1(\hat{z}, t)\mathcal{E}_2^*(\hat{z}, t)|2\rangle\langle 1| + \mathcal{E}_1^*(\hat{z}, t)\mathcal{E}_2(\hat{z}, t)|1\rangle\langle 2|\right]$$

Atom interferometers.

Quantise centre-of-mass motion in $z-$ direction:

$$H = \hbar g \left[\mathcal{E}_1(\hat{z},t)\mathcal{E}_2^*(\hat{z},t)|2\rangle\langle 1| + \mathcal{E}_1^*(\hat{z},t)\mathcal{E}_2(\hat{z},t)|1\rangle\langle 2|\right]$$

$$\mathcal{E}_j(\hat{z},t) = \mathcal{E}_0 e^{-i(\omega_1 t - k_j \hat{z})}$$

with $k_2 = -k_1$.

Atom interferometers.

Quantise centre-of-mass motion in $z-$ direction:

$$H = \hbar g \left[\mathcal{E}_1(\hat{z},t)\mathcal{E}_2^*(\hat{z},t)|2\rangle\langle 1| + \mathcal{E}_1^*(\hat{z},t)\mathcal{E}_2(\hat{z},t)|1\rangle\langle 2|\right]$$

$$\mathcal{E}_j(\hat{z},t) = \mathcal{E}_0 e^{-i(\omega_1 t - k_j\hat{z})}$$

with $k_2 = -k_1$.

$$e^{-i\alpha\hat{z}}\hat{p}_z e^{i\alpha\hat{z}} = \hat{p}_z + \hbar\alpha$$

Atom interferometers.

Quantise centre-of-mass motion in $z-$ direction:

$$H = \hbar g \left[\mathcal{E}_1(\hat{z},t)\mathcal{E}_2^*(\hat{z},t)|2\rangle\langle 1| + \mathcal{E}_1^*(\hat{z},t)\mathcal{E}_2(\hat{z},t)|1\rangle\langle 2|\right]$$

$$\mathcal{E}_j(\hat{z},t) = \mathcal{E}_0 e^{-i(\omega_1 t - k_j\hat{z})}$$

with $k_2 = -k_1$.

$$e^{-i\alpha\hat{z}}\hat{p}_z e^{i\alpha\hat{z}} = \hat{p}_z + \hbar\alpha$$

$$e^{i\alpha\hat{z}}|p\rangle = |p + \hbar\alpha\rangle$$

Atom interferometers.

On Raman resonance $\omega_A = \omega_1 - \omega_2$

$$H = \hbar g \left[e^{i\Delta k \hat{z}} |2\rangle\langle 1| + e^{-i\Delta k \hat{z}} |1\rangle\langle 2| \right]$$

$\Delta = k_1 + k_2$

Atom interferometers.

On Raman resonance $\omega_A = \omega_1 - \omega_2$

$$H = \hbar g \left[e^{i\Delta k\hat{z}}|2\rangle\langle 1| + e^{-i\Delta k\hat{z}}|1\rangle\langle 2| \right]$$

$\Delta = k_1 + k_2$

$$\begin{aligned} H|p,1\rangle &= |p+\hbar\Delta,2\rangle \\ H|p,2\rangle &= |p-\hbar\Delta,1\rangle \end{aligned}$$

excited state has $2\hbar(k_1 + k_2)$ more momentum than the ground state.

Atom interferometers.

On Raman resonance $\omega_A = \omega_1 - \omega_2$

$$H = \hbar g \left[e^{i\Delta k\hat{z}} |2\rangle\langle 1| + e^{-i\Delta k\hat{z}} |1\rangle\langle 2| \right]$$

$\Delta = k_1 + k_2$

$$\begin{aligned} H|p,1\rangle &= |p + \hbar\Delta, 2\rangle \\ H|p,2\rangle &= |p - \hbar\Delta, 1\rangle \end{aligned}$$

excited state has $2\hbar(k_1 + k_2)$ more momentum than the ground state.

Usually $|1\rangle, |2\rangle$ are hyperfine ground states. $\omega_A << \omega_{1,2}$

Atom interferometers.

$$U(\theta) = \exp\left[-i\frac{\theta}{2}(e^{-i\Delta\hat{z}}\sigma_+ + e^{i\Delta\hat{z}}\sigma_-)\right]$$

Atom interferometers.

$$U(\theta) = \exp\left[-i\frac{\theta}{2}(e^{-i\Delta\hat{z}}\sigma_+ + e^{i\Delta\hat{z}}\sigma_-)\right]$$

$$\begin{aligned} U(\theta)|k,1\rangle &= \cos\theta/2|k,1\rangle - i\sin\theta/2|k+\Delta,2\rangle \\ U(\theta)|k,2\rangle &= \cos\theta/2|k,2\rangle - i\sin\theta/2|k-\Delta,1\rangle \end{aligned}$$

Atom interferometers.

Kasevich and Chu, PRL (1991).

Atom interferometers.

Kasevich and Chu, PRL (1991).

$\pi/2$ — π — $\pi/2$ pulse sequence.

Atom interferometers.

Kasevich and Chu, PRL (1991).

$\pi/2$ — π — $\pi/2$ pulse sequence.

$\pi/2$ pulse:

$$|k,1\rangle \rightarrow \frac{1}{\sqrt{2}}(|k,1\rangle - i|k+\Delta,2\rangle)$$

$$|k,2\rangle \rightarrow \frac{1}{\sqrt{2}}(|k,2\rangle - i|k-\Delta,1\rangle)$$

Atom interferometers.

Kasevich and Chu, PRL (1991).

$\pi/2$ — π — $\pi/2$ pulse sequence.

$\pi/2$ pulse:

$$|k,1\rangle \rightarrow \frac{1}{\sqrt{2}}(|k,1\rangle - i|k+\Delta,2\rangle)$$

$$|k,2\rangle \rightarrow \frac{1}{\sqrt{2}}(|k,2\rangle - i|k-\Delta,1\rangle)$$

π pulse:

$$|k,1\rangle \rightarrow -i|k+\Delta,2\rangle)$$

$$|k+\Delta,2\rangle \rightarrow -i|k,1\rangle)$$

Atom interferometers.

Kasevich and Chu, PRL (1991).

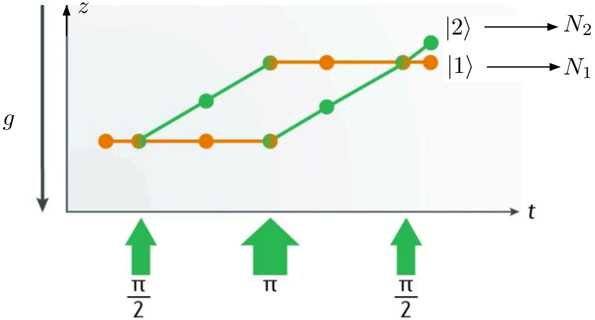

What is the phase difference between the two paths for CoM motion?

Atom interferometers.

See https://arxiv.org/pdf/0806.3261.pdf

$$\Delta\phi = \Delta\phi_{propagation} + \Delta\phi_{separation} + \Delta\phi_{laser}$$

Atom interferometers.

The propagation phase $\Delta\phi_{propagation}$ due to free–fall evolution of the atom between light pulses:

$$\Delta\phi_{propagation} = \sum_{upper} \int_{t_I}^{t_F} (L_c - E_i)dt - \sum_{lower} \int_{t_I}^{t_F} (L_c - E_i)dt$$

Sums over path segments of the upper and lower arms,

L_c is the classical Lagrangian evaluated along the classical trajectory of each path segment.

contribution from the internal atomic energy level E_i.

t_I and t_F and L_c and E_i, depend on the path segment.

Atom interferometers.

$$\Delta\phi_{laser} = \left(\sum_j \pm\phi_L(t_j, \vec{x}_u(t_j))\right)_{upper} - \left(\sum_j \pm\phi_L(t_j, \vec{x}_l(t_j))\right)_{lower}$$

$$\phi_L(t_0, \vec{x}_c(t_0)) = \vec{k}. \cdot \vec{x}_c(t_0) - \omega t_0 + \phi$$

Comes from the interaction of the atom with the laser field used to manipulate the wave function at each of the beamsplitters and mirrors in the interferometer.

Sum over all the interaction points at the times t_j, and $\vec{x}_u(t)$ and $\vec{x}_l(t)$are the classical trajectories of the upper and lower arm of the interferometer, respectively.

The sign of each term depends on whether the atom gains $(+)$ or loses $(-)$ momentum as a result of the interaction.

Atom interferometers.

The separation phase $\Delta\phi_{separation}$ arises when the classical trajectories of the two arms of the interferometer do not exactly intersect at the final beamsplitter.

Atom interferometers:inertial applications.

The optical phase shifts dominate, $\Delta\phi_{tot} \approx \Delta\phi_{laser}$, independent of the output port of the interferometer.

Atom interferometers: gyroscope.

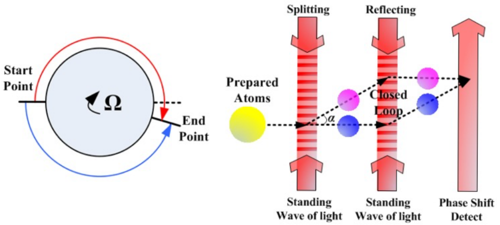

Atom interferometers: gyroscope.

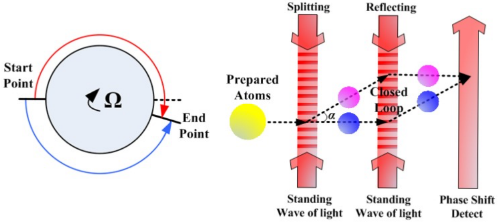

Gyroscope. atoms have initial velocity $\vec{v}_0$ and Raman propagation vectors initially have common orientations $\vec{k}_0$ which rotate with angular rate $\vec{\Omega}$

$$\Delta\phi_{laser} \approx \vec{k}_0 \cdot (2\vec{v}_0 \times \vec{\Omega})T^2$$

T interogation time inside the interferometer. Example: length 8.8m, $T = 1.34$s.

Atom interferometers: gyroscope.

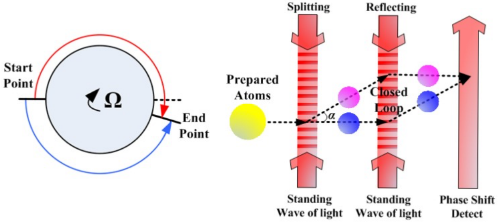

Gyroscope. atoms have initial velocity $\vec{v}_0$ and Raman propagation vectors initially have common orientations $\vec{k}_0$ which rotate with angular rate $\vec{\Omega}$

$$\Delta\phi_{laser} \approx \vec{k}_0 \cdot (2\vec{v}_0 \times \vec{\Omega}) T^2$$

T interogation time inside the interferometer. Example: length 8.8m, $T = 1.34$s.
In principle, AIG is more sensitive to rotation by a factor of 10^{10} than optical gyroscope of the same area. Usually area is much less than optical gyro.

Atom interferometers:inertial applications.

accelerometers.

$$\Delta\phi_{laser} = \vec{k}_0 \cdot \vec{a} T^2$$

Atom interferometers:inertial applications.

accelerometers.

$$\Delta\phi_{laser} = \vec{k}_0 \cdot \vec{a} T^2$$

stationary interferometer, with the laser beams vertically directed, measures the acceleration due to gravity.

Atom interferometers:inertial applications.

accelerometers.

$$\Delta\phi_{laser} = \vec{k}_0 \cdot \vec{a} T^2$$

stationary interferometer, with the laser beams vertically directed, measures the acceleration due to gravity.

Compact, geophysical (10^{-8}g accuracy) instruments should enable low cost gravity field surveys.

Atom interferometers:inertial applications.

accelerometers.

$$\Delta\phi_{laser} = \vec{k}_0 \cdot \vec{a} T^2$$

stationary interferometer, with the laser beams vertically directed, measures the acceleration due to gravity.

Compact, geophysical (10^{-8}g accuracy) instruments should enable low cost gravity field surveys.

Real-world environments: external interference, platform noise, and constraints on size, weight, and power.
Tailored light pulses designed using robust control techniques (Q-CTRL, Sydney)) mitigate significant error sources in an atom-interferometric accelerometer and give a factor of 21 enhancement .
`https://doi.org/10.1038/s41467-023-43374-0`

Atom interferometers:inertial applications.

Gravity gradiometer: measures changes in the acceleration due to gravity over fixed baselines.

Atom interferometers:inertial applications.

Gravity gradiometer: measures changes in the acceleration due to gravity over fixed baselines.

Pairs of interforemeters separated vertically.

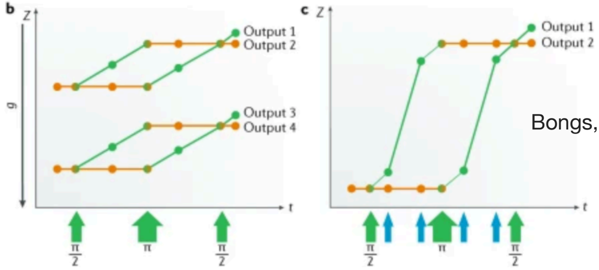

Bongs, K., *et al.* *Nat Rev Phys* **1**, (2019).

Additional laser pulses (blue arrows) increase the spacetime area of the atom interferometer enhancing the sensitivity.

Atom interferometers:inertial applications.

Gravity gradiometers have applications in geodesy and oil/mineral exploration.

Measure changes in G at 3×10^{-4} level.